

# Upper horizontal blades (n=56) June

# blade,	ystart,	center pos,	angle,	yend	# blade,	ystart,	center pos,	angle,	yend
1	1.319364	1.341147	0.072483	1.362930	29	0.388608	0.397525	0.029716	0.406443
2	1.270368	1.291479	0.070257	1.312591	30	0.368021	0.376652	0.028761	0.385283
3	1.222878	1.243339	0.068095	1.263799	31	0.348059	0.356412	0.027835	0.364764
4	1.176848	1.196676	0.065998	1.216504	32	0.328702	0.336785	0.026937	0.344869
5	1.132230	1.151445	0.063962	1.170660	33	0.309933	0.317754	0.026066	0.325576
6	1.088981	1.107600	0.061986	1.126220	34	0.291732	0.299300	0.025222	0.306868
7	1.047056	1.065099	0.060068	1.083140	35	0.274083	0.281405	0.024402	0.288727
8	1.006415	1.023897	0.058207	1.041379	36	0.256969	0.264053	0.023608	0.271137
9	0.967018	0.983956	0.056401	1.000895	37	0.240374	0.247227	0.022837	0.254079
10	0.928825	0.945236	0.054649	0.961647	38	0.224282	0.230910	0.022090	0.237538
11	0.891799	0.907698	0.052948	0.923598	39	0.208677	0.215088	0.021365	0.221498
12	0.855904	0.871307	0.051299	0.886710	40	0.193545	0.199745	0.020662	0.205944
13	0.821103	0.836025	0.049698	0.850947	41	0.178872	0.184867	0.019980	0.190862
14	0.787365	0.801820	0.048145	0.816274	42	0.164643	0.170440	0.019319	0.176236
15	0.754655	0.768656	0.046638	0.782658	43	0.150845	0.156449	0.018678	0.162053
16	0.722942	0.736504	0.045176	0.750066	44	0.137465	0.142883	0.018056	0.148300
17	0.692194	0.705330	0.043758	0.718466	45	0.124491	0.129727	0.017453	0.134963
18	0.662383	0.675105	0.042382	0.687827	46	0.111909	0.116970	0.016868	0.122031
19	0.633479	0.645800	0.041048	0.658121	47	0.099708	0.104599	0.016301	0.109489
20	0.605454	0.617386	0.039753	0.629318	48	0.087877	0.092602	0.015751	0.097328
21	0.578282	0.589836	0.038497	0.601391	49	0.076404	0.080969	0.015217	0.085535
22	0.551935	0.563124	0.037279	0.574313	50	0.065278	0.069688	0.014700	0.074098
23	0.526389	0.537223	0.036097	0.548057	51	0.054489	0.058749	0.014198	0.063008
24	0.501620	0.512109	0.034951	0.522599	52	0.044027	0.048140	0.013711	0.052254
25	0.477603	0.487758	0.033839	0.497914	53	0.033881	0.037853	0.013239	0.041825
26	0.454315	0.464147	0.032760	0.473978	54	0.024043	0.027877	0.012782	0.031712
27	0.431734	0.441252	0.031714	0.450769	55	0.014502	0.018204	0.012338	0.021905
28	0.409839	0.419052	0.030700	0.428264	56	0.005250	0.008823	0.011908	0.012395

## Lower horizontal blades (n=37) June

# bladel, ystart, center pos, angle, yend

1	-0.909727	-0.918920	-0.030633	-0.928113
2	-0.886993	-0.895869	-0.029579	-0.904746
3	-0.864949	-0.873518	-0.028557	-0.882088
4	-0.843573	-0.851845	-0.027566	-0.860117
5	-0.822846	-0.830830	-0.026605	-0.838813
6	-0.802748	-0.810452	-0.025673	-0.818155
7	-0.783260	-0.790692	-0.024768	-0.798124
8	-0.764362	-0.771531	-0.023891	-0.778700
9	-0.746037	-0.752951	-0.023041	-0.759864
10	-0.728268	-0.734934	-0.022216	-0.741600
11	-0.711037	-0.717463	-0.021415	-0.723889
12	-0.694329	-0.700522	-0.020639	-0.706714
13	-0.678127	-0.684094	-0.019887	-0.690060
14	-0.662416	-0.668163	-0.019157	-0.673911
15	-0.647180	-0.652716	-0.018449	-0.658251
16	-0.632407	-0.637736	-0.017762	-0.643065
17	-0.618080	-0.623210	-0.017097	-0.628339
18	-0.604188	-0.609124	-0.016451	-0.614060
19	-0.590717	-0.595464	-0.015825	-0.600212
20	-0.577653	-0.582219	-0.015217	-0.586784

# bladel, ystart, center pos, angle, yend

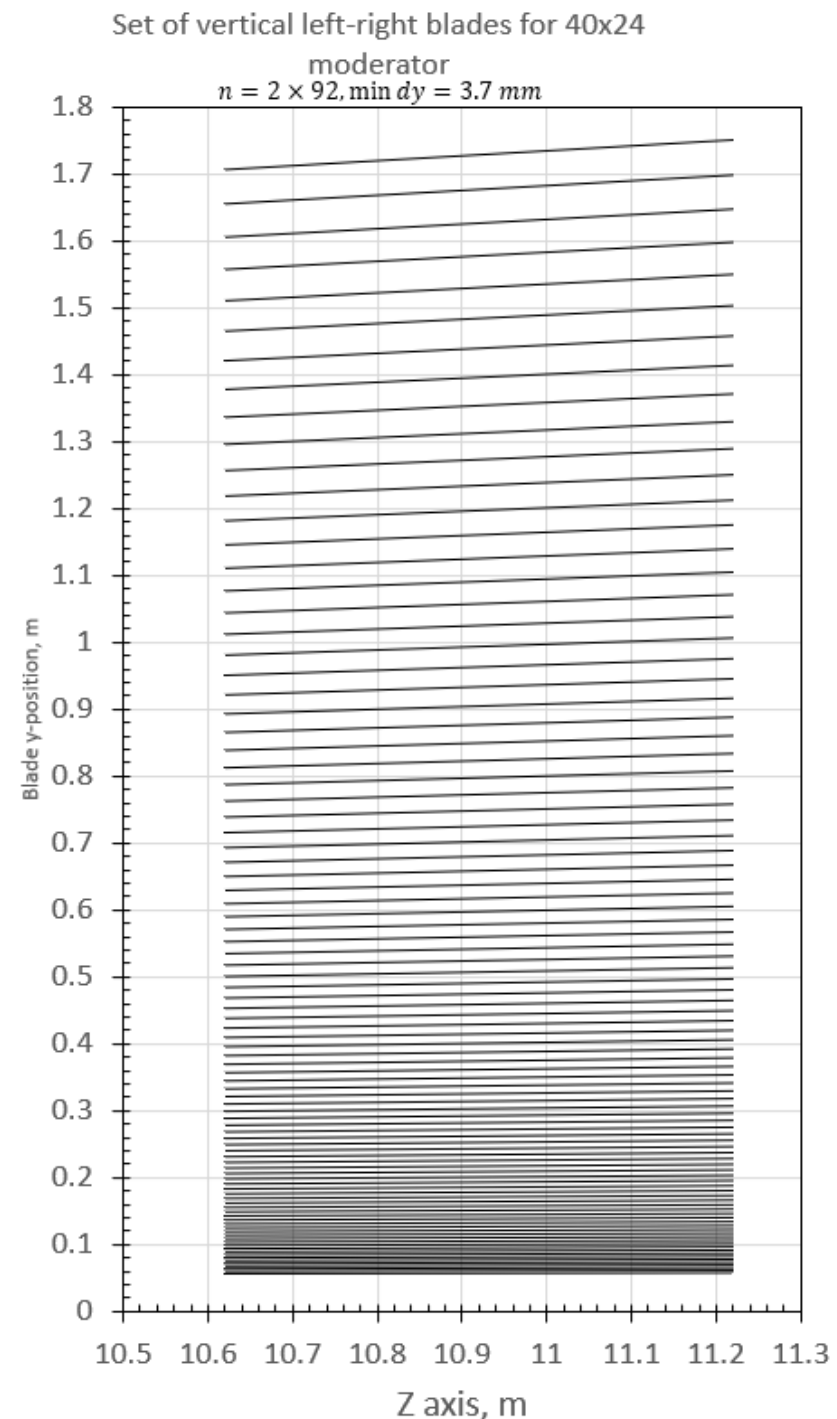
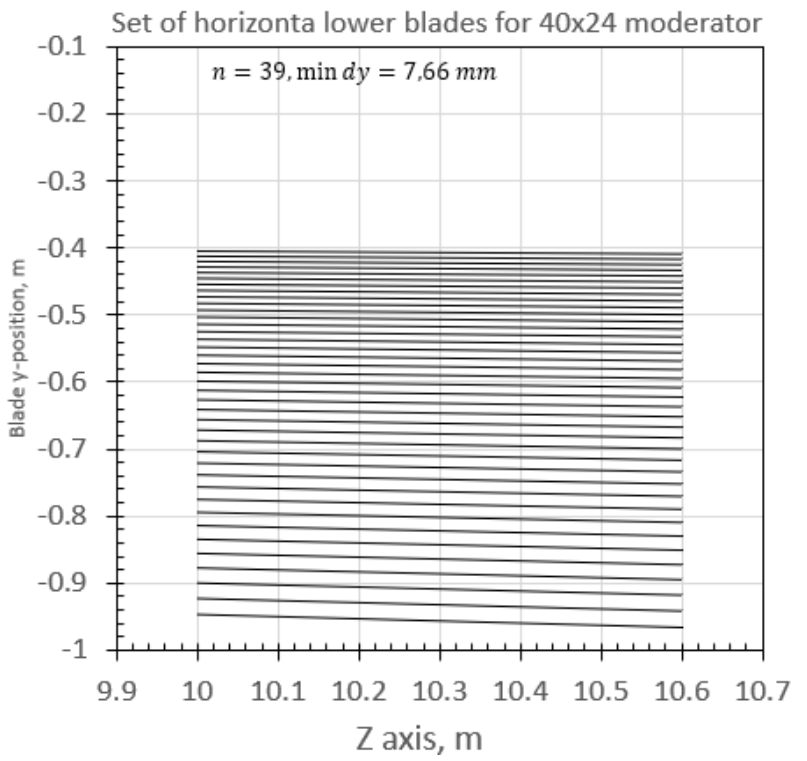
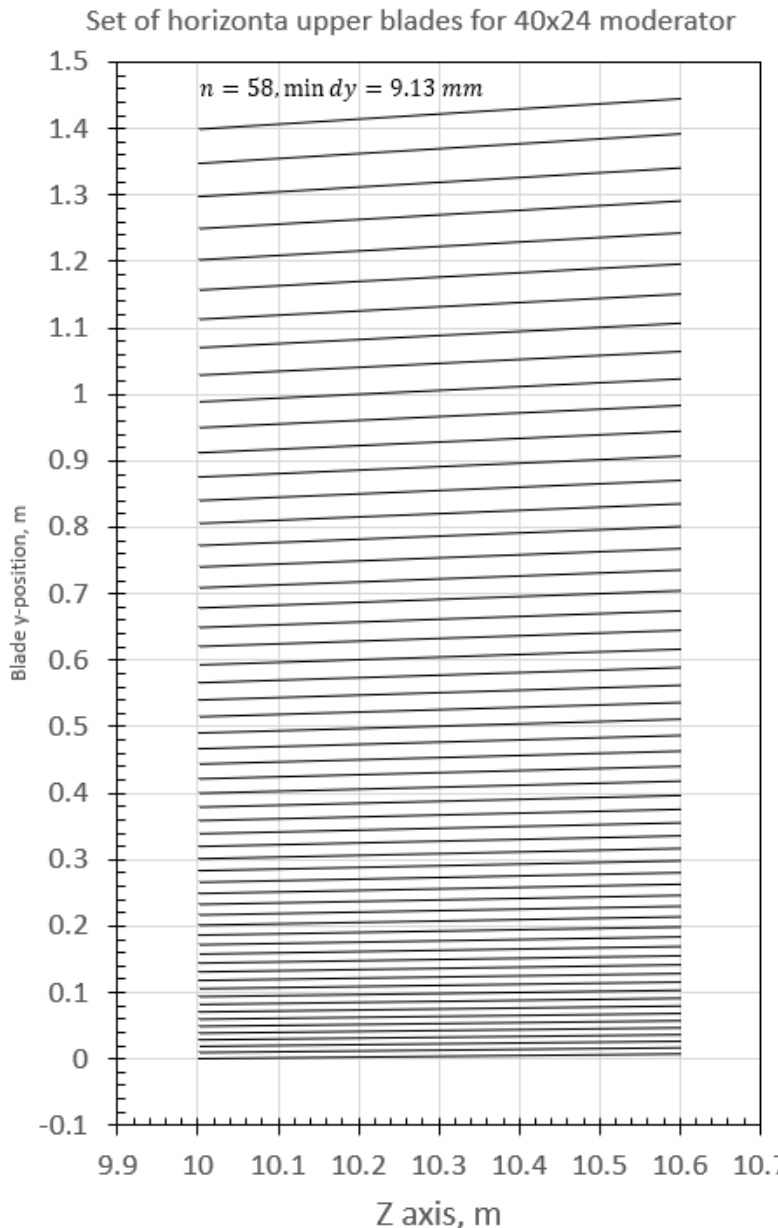
21	-0.564985	-0.569374	-0.014628	-0.573763
22	-0.552701	-0.556918	-0.014057	-0.561135
23	-0.540788	-0.544839	-0.013503	-0.548891
24	-0.529236	-0.533126	-0.012966	-0.537016
25	-0.518034	-0.521768	-0.012445	-0.525502
26	-0.507171	-0.510754	-0.011940	-0.514336
27	-0.496637	-0.500072	-0.011450	-0.503507
28	-0.486422	-0.489715	-0.010974	-0.493007
29	-0.476516	-0.479670	-0.010514	-0.482824
30	-0.466910	-0.469930	-0.010067	-0.472950
31	-0.457594	-0.460484	-0.009633	-0.463375
32	-0.448561	-0.451325	-0.009213	-0.454089
33	-0.439801	-0.442442	-0.008805	-0.445084
34	-0.431306	-0.433829	-0.008410	-0.436352
35	-0.423068	-0.425476	-0.008027	-0.427884
36	-0.415079	-0.417376	-0.007655	-0.419673
37	-0.407333	-0.409521	-0.007295	-0.411709

# Vertical blades (n=91) June

# blade,	ystart,	center pos,	angle,	length	end	# blade,	ystart,	center pos,	angle,	length	end
1	1.618916	1.640010	0.070198	0.601481	1.661105	80	0.099657	0.100963	0.004356	0.600006	0.102270
2	1.570275	1.590743	0.068121	0.601395	1.611211	81	0.094801	0.096044	0.004144	0.600005	0.097287
3	1.523050	1.542910	0.066101	0.601313	1.562769	82	0.090085	0.091266	0.003937	0.600005	0.092447
4	1.477198	1.496466	0.064138	0.601236	1.515734	83	0.085503	0.086625	0.003737	0.600004	0.087746
5	1.432679	1.451372	0.062230	0.601164	1.470065	84	0.081053	0.082116	0.003543	0.600004	0.083179
6	1.389452	1.407586	0.060374	0.601095	1.425721	85	0.076731	0.077737	0.003354	0.600003	0.078743
7	1.347479	1.365070	0.058571	0.601031	1.382662	86	0.072532	0.073483	0.003170	0.600003	0.074435
8	1.306723	1.323786	0.056818	0.600970	1.340850	87	0.068454	0.069352	0.002992	0.600003	0.070249
9	1.267147	1.283698	0.055114	0.600912	1.300249	88	0.064493	0.065338	0.002819	0.600002	0.066184
10	1.228717	1.244770	0.053458	0.600858	1.260823	89	0.060645	0.061440	0.002651	0.600002	0.062235
11	1.191399	1.206968	0.051849	0.600807	1.222536	90	0.056907	0.057653	0.002487	0.600002	0.058399
12	1.155160	1.170258	0.050285	0.600759	1.185356	91	0.053277	0.053975	0.002329	0.600002	0.054674
13	1.119968	1.134609	0.048765	0.600714	1.149251						
14	1.085793	1.099990	0.047288	0.600672	1.114187						
15	1.052605	1.066370	0.045852	0.600631	1.080136						
16	1.020374	1.033720	0.044457	0.600593	1.047066						
17	0.989074	1.002012	0.043102	0.600558	1.014951						
18	0.958675	0.971218	0.041785	0.600524	0.983761						
19	0.929153	0.941311	0.040505	0.600493	0.953470						
20	0.900482	0.912266	0.039261	0.600463	0.924051						
21	0.872636	0.884058	0.038053	0.600435	0.895479						
22	0.845592	0.856661	0.036879	0.600408	0.867730						
23	0.819327	0.830053	0.035738	0.600383	0.840779						
24	0.793818	0.804211	0.034630	0.600360	0.814604						
25	0.769042	0.779112	0.033553	0.600338	0.789182						
26	0.744979	0.754735	0.032507	0.600317	0.764490						
27	0.721609	0.731059	0.031490	0.600298	0.740509						
28	0.698910	0.708063	0.030503	0.600279	0.717217						
29	0.676863	0.685729	0.029543	0.600262	0.694594						
30	0.655450	0.664036	0.028611	0.600246	0.672622						

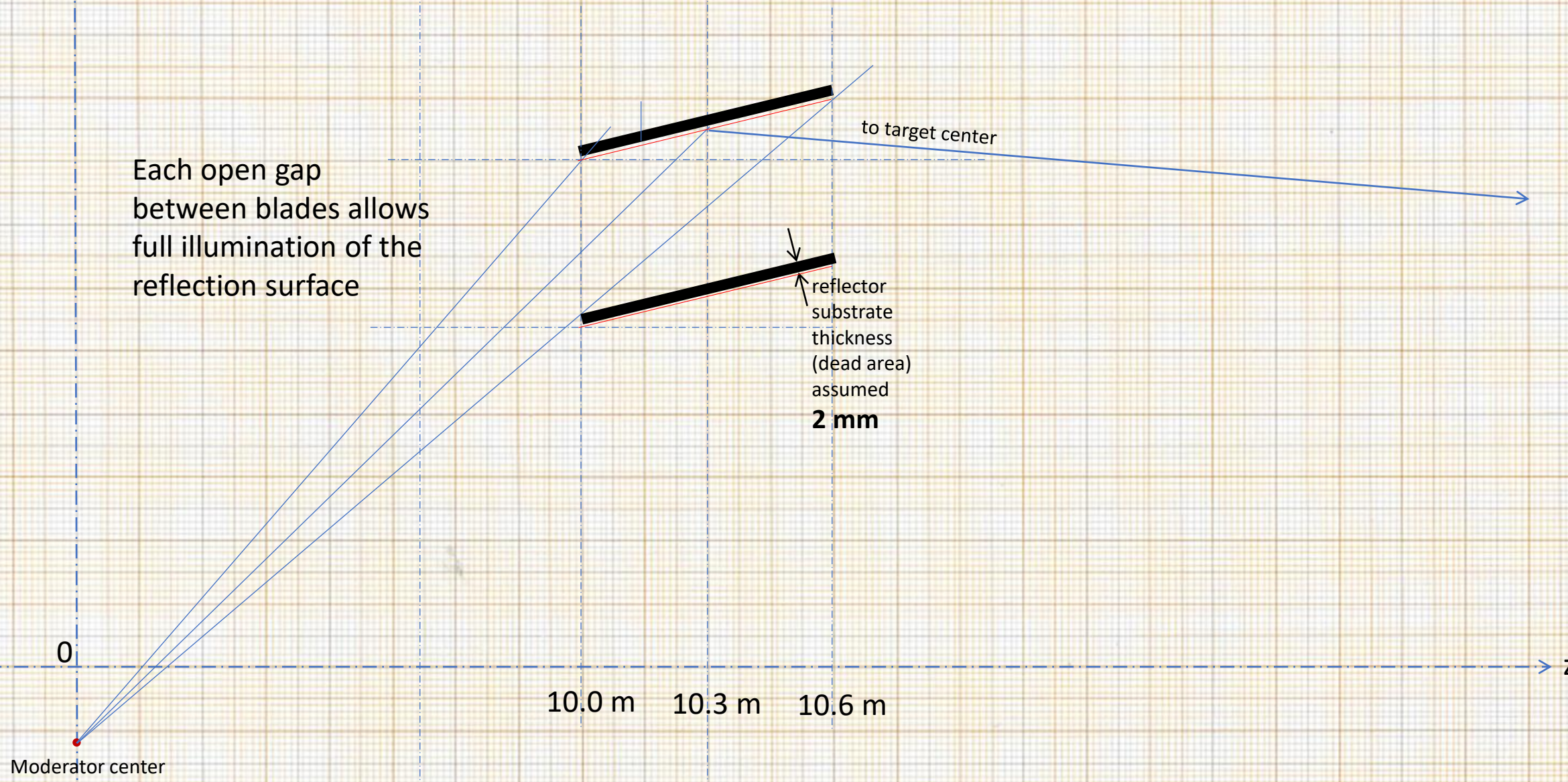
xminlow = 0.05175 m

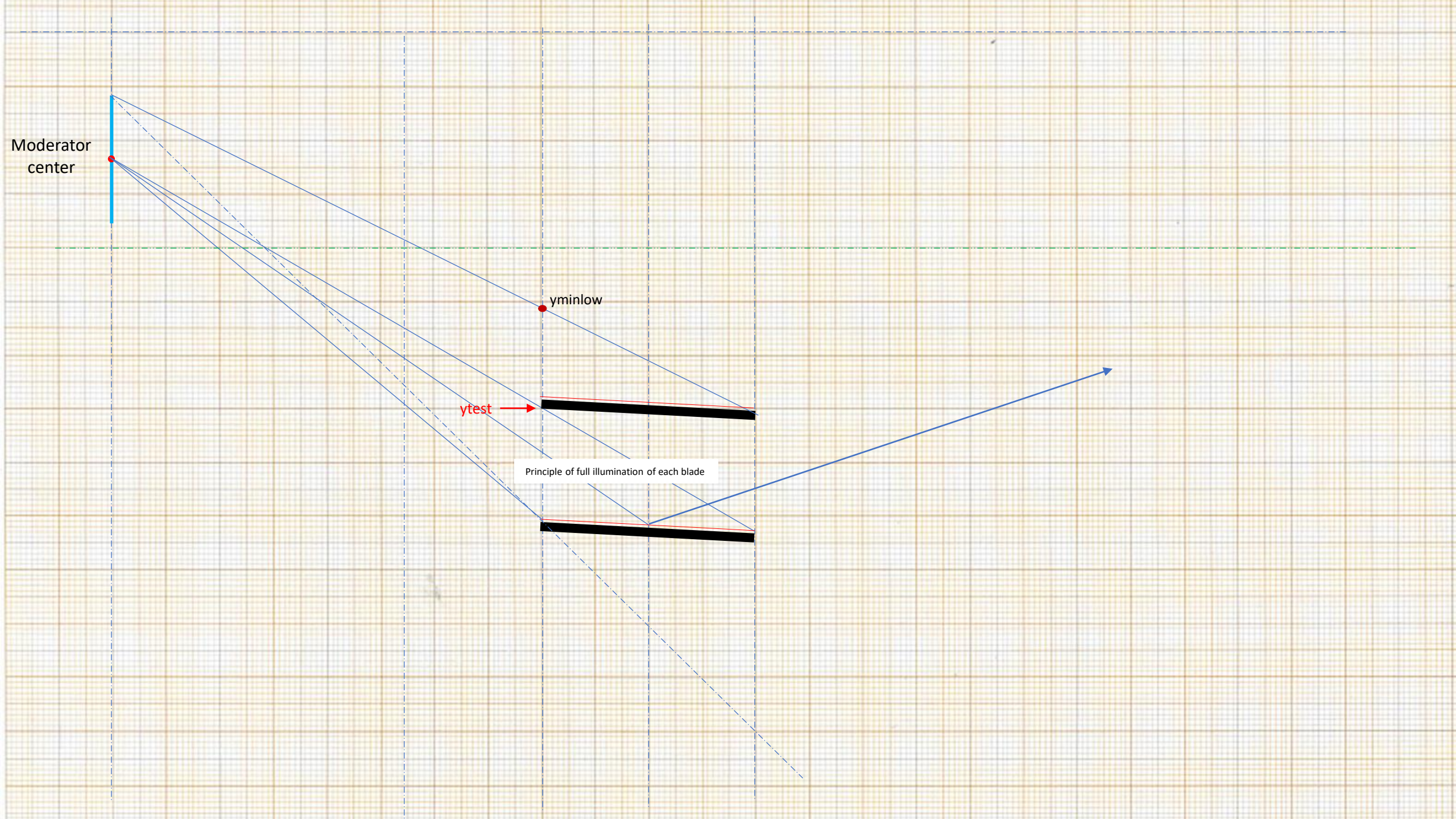
# Blades map Sept 18, 2022, for 40x24 LD2 but emitting from 0.25 m



y

## Construction of the blade sets of venetian-blinds reflector





Y

Where events sneak into horizontal line in the detector for the point-like source

Moderator  
center



-0.1

-0.2

-0.3

-0.4

-0.5

*Direction from the center of moderator that gives additional line in the detector*

35 -0.423068 -0.425476 -0.008027 0.600019 -0.427884

36 -0.415079 -0.417376 -0.007655 0.600018 -0.419673

37 -0.407333 -0.409521 -0.007295 0.600016 -0.411709

y

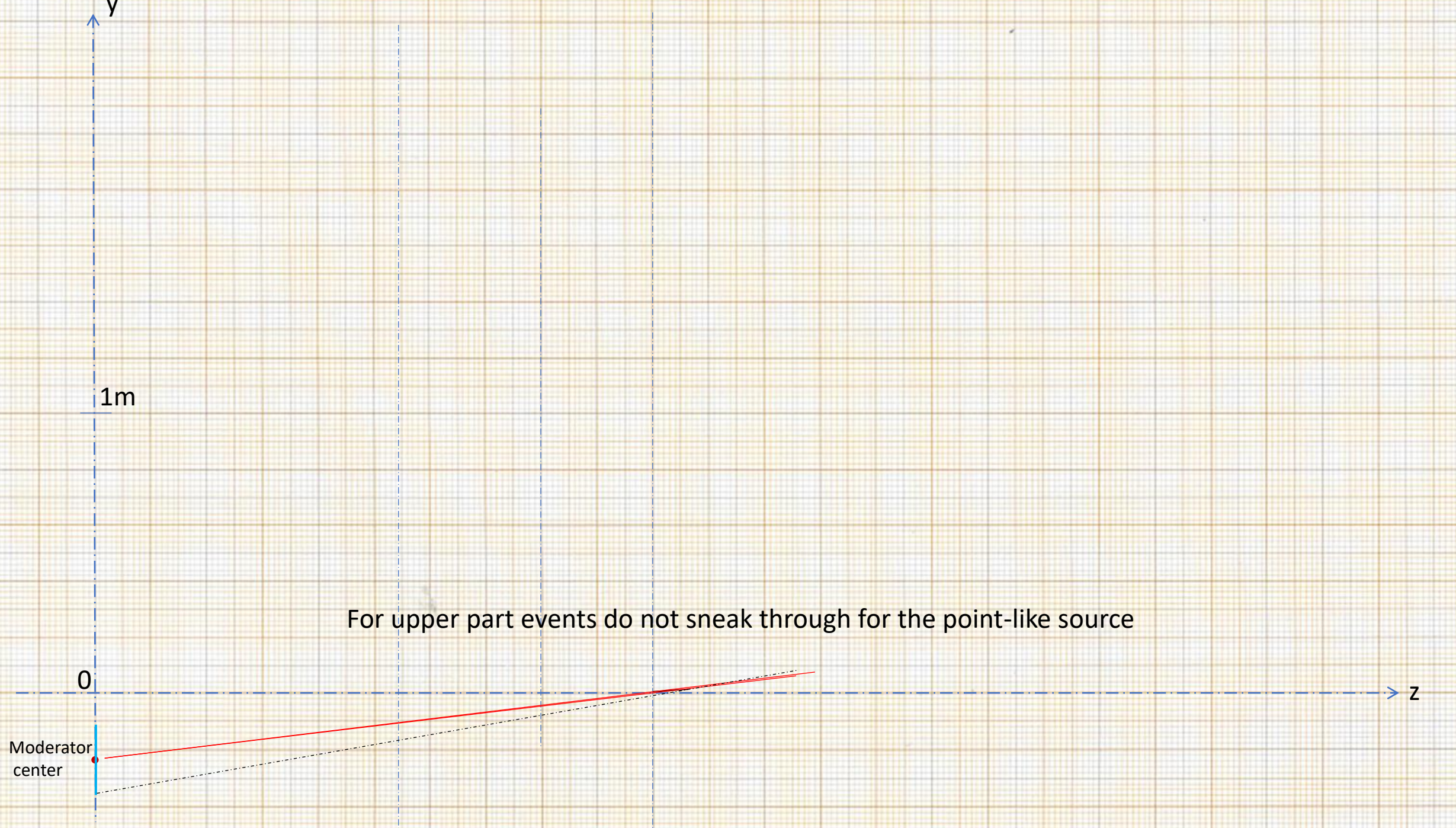
1m

z

For upper part events do not sneak through for the point-like source

0

Moderator  
center



X (top view on vertical blades)

2m

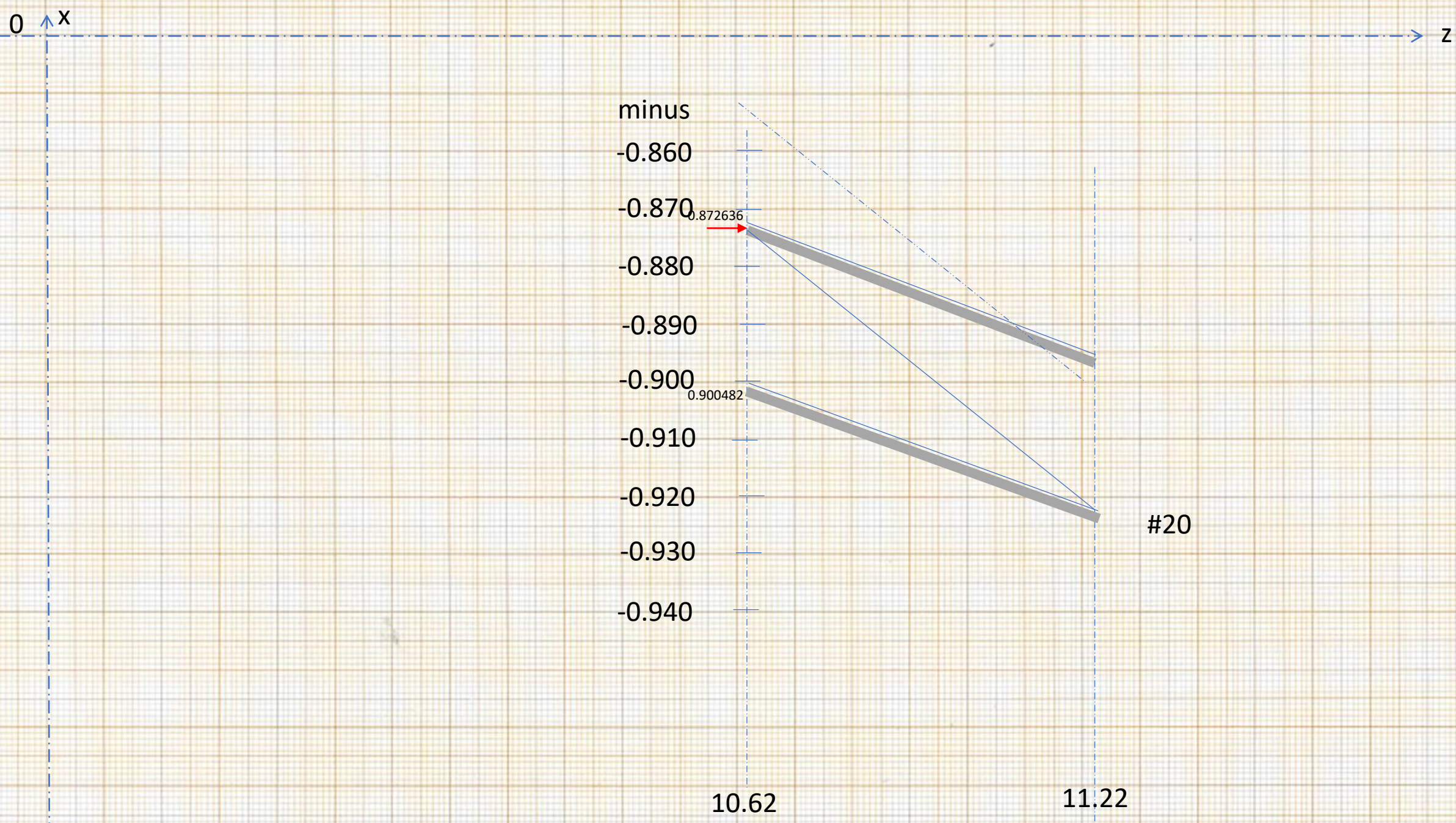
1m

Moderator  
center 0

z

to target center





x

0

z

1.160

1.150  
0.872636

1.140

1.130

1.120  
0.900482

1.110

1.100

1.090

1.080

10.62

11.22

#13 OK



```
write(6,*)'OXV',nprint,XE2,YE2,ZE2,VX,VY,VZ
```

```
write(6,*)nk, delpox(nk), beta, xbn, deno, ztoc, ZC2
```

	<b>XE2</b>	<b>ZE2</b>	<b>VX</b>	<b>VZ</b>		
1	-0.136595696	0.825501978	10.6199999	-12.4078836	-5.10144806	969.738586
73	6.02716208E-03	6.02723518E-03	0.137901545	-1.88223161E-02	-14.5836058	-3.96360588

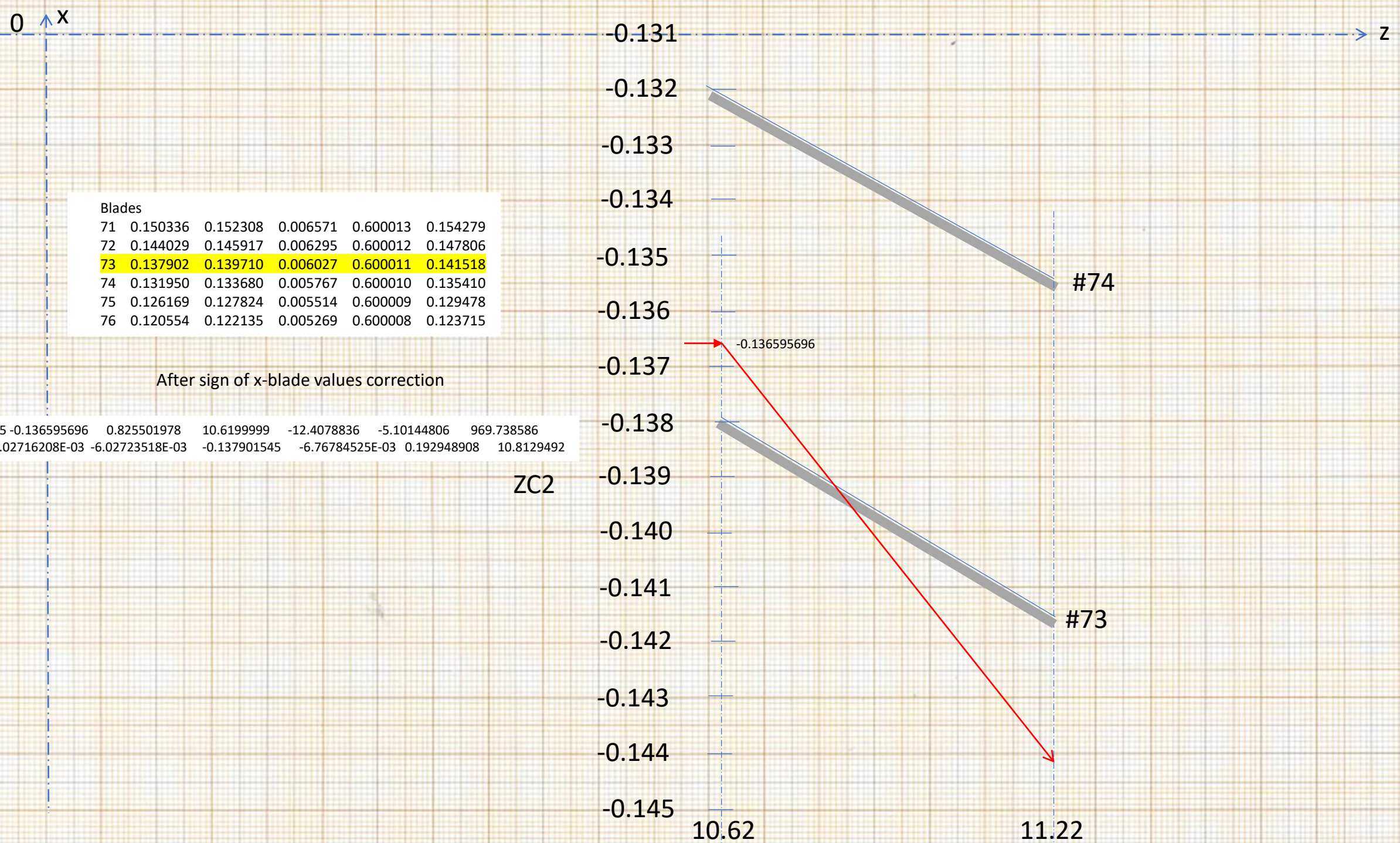
Blades

71	0.150336	0.152308	0.006571	0.600013	0.154279
72	0.144029	0.145917	0.006295	0.600012	0.147806
73	0.137902	0.139710	0.006027	0.600011	0.141518
74	0.131950	0.133680	0.005767	0.600010	0.135410
75	0.126169	0.127824	0.005514	0.600009	0.129478
76	0.120554	0.122135	0.005269	0.600008	0.123715

**XE2 .ne. ZE2\*VX/VZ**  
if reflection occurs in  
the first horizontal pack

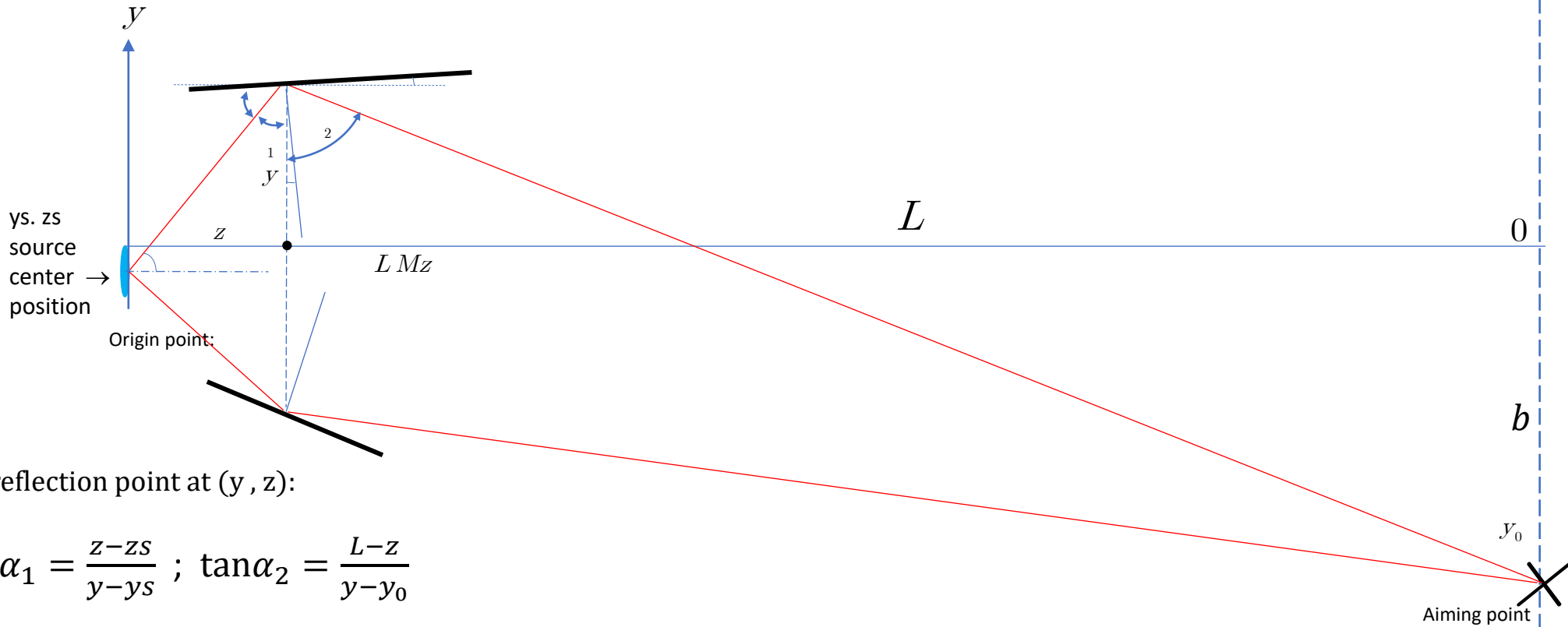
Negative crossing  
point is still an error;  
It should be between  
10.62 and 11.22

Resolved:  
see next slide



# Reflector geometry

only vertical plane, no gravity



For reflection point at  $(y, z)$ :

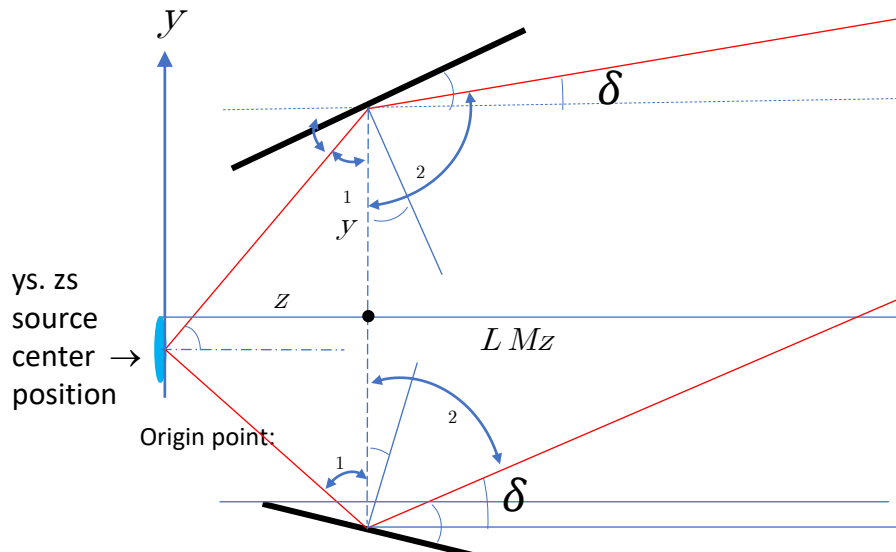
$$\tan \alpha_1 = \frac{z - z_s}{y - y_s} ; \tan \alpha_2 = \frac{L - z}{y - y_0}$$

Note, both  $y_s$  and  $y_0$  are negative

$$\alpha_1 + \beta = \alpha_2 - \beta; \quad \beta = \frac{\alpha_2 - \alpha_1}{2}$$

# Reflector geometry

only vertical plane, no gravity

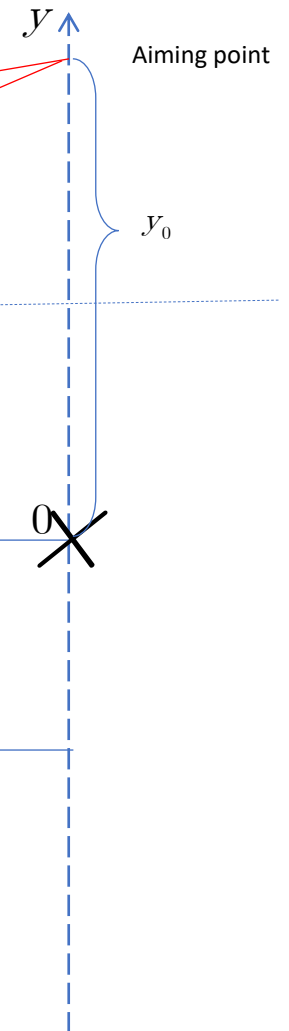


For reflection point at  $(y, z)$ :

$$\tan \alpha_1 = \frac{z - z_s}{y - y_s}$$

$$\begin{aligned}\tan \delta &= (y_0 - y)/(L - z) \\ \delta &= \text{atan}(\tan \delta) \\ \alpha_2 &= 90^\circ + \delta\end{aligned}$$

$$\alpha_1 + \beta = \alpha_2 - \beta; \quad \beta = \frac{\alpha_2 - \alpha_1}{2}$$



# Summary / Result

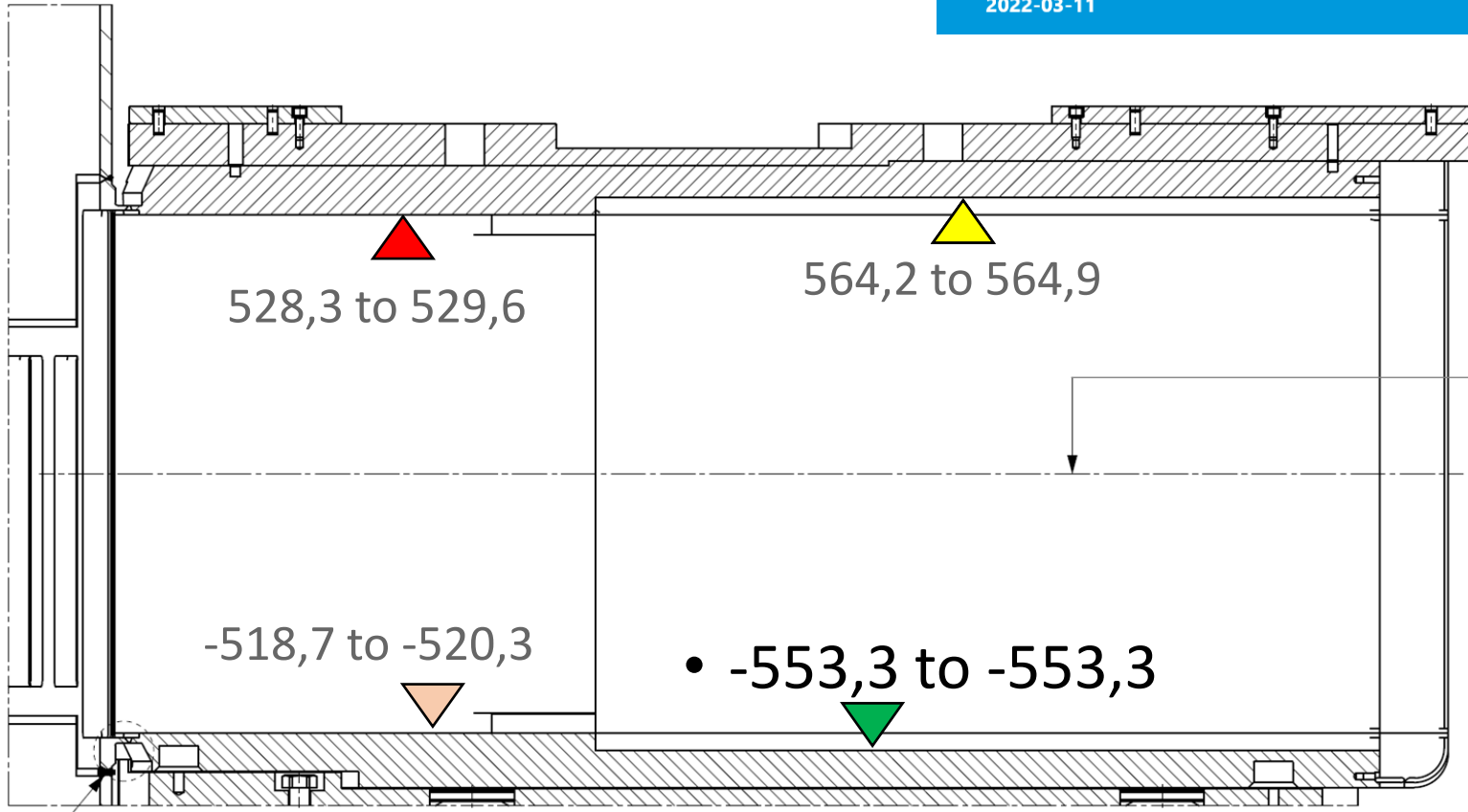
Estimated As Built Z-levels

## NNbar Frame Z Levels

ESS-4001838

BY KRSITER BLOMBERG

2022-03-11



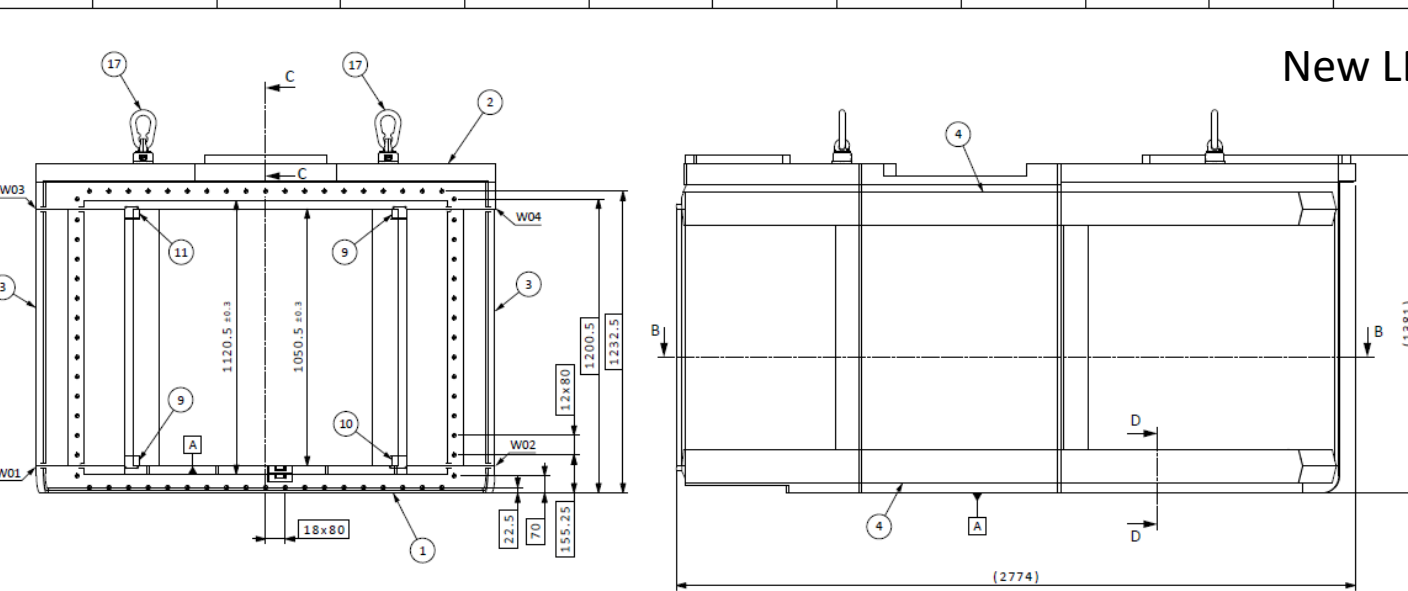
TCS-Z = 0

Vertical LBP opening :

$$+564.9 - (-553.3) = 1118.8 \text{ mm}$$

or  $\pm 5.81^\circ$  (1119.3 mm)

New LBP; May 2022



**NOTE \*:**  
**THIS SURFACE TO BE MACHINED AND THR**

WELD 01-04 TO BE PERFORMED ACCORDING  
DOCUMENTED ON WELD LIST

**COMPONENT 1-3 WELDED ACCORDING TO  
ALONG ALL 4 EDGES**

NN-BAR PORT SHALL HAVE A SURFACE FIN  
INTERIOR SURFACES

SHARP EDGES BROKEN  
PARALLEL PINS SHOULD HAVE A SMALL GRIT TO PREVENT TRAPPED AIR

**INTERNAL PORTS TO BE CHECKED AND CLEANED  
ADDITIONAL ASSEMBLY**

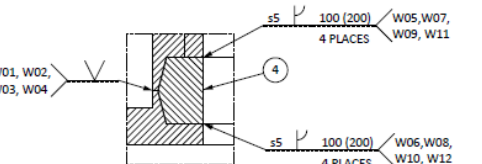
NNBAR TUBE TO BE LIFTED WITH SPREADER  
LIFTING POINTS IS LOADED VERTICALLY  
  
INSPECTION PLAN FOR ASSEMBLY ESS-033  
QUALITY CLASS MOC4A

DESIGN PRESSURE: 1 BAR(g) / VACUUM  
TEST PRESSURE: 1,43 BAR(g)  
  
MEDIA: VACUUM  
TEST GROUP: 3B  
PED.KAT. IV MODUL G

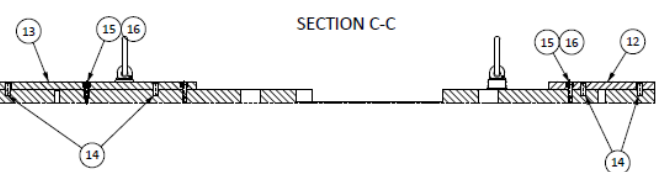
Part Number	Qty	CAB Number	Title
THIS IS A SUPPLEMENT TO <b>NBNBAR FRAME</b> SYSTEM 105B			
E55-0081156	1	E55-0081156	UPMING POINT M3X100
E55-0081157	1	E55-0081157	WASHER
E55-01351947	1	E55-01351947	HEXAGON ALLEN HEAD
E55-02232006	6	E55-02232006	PIN
E55-02232007	1	E55-02232007	FLUKE BAR LOW
E55-02232008	1	E55-02232008	FLUKE BAR HIGH
E55-02232010	1	E55-02232010	FILLER WEDGE NO. 3
E55-02232011	1	E55-02232011	FILLER WEDGE NO. 2
E55-02232012	1	E55-02232012	FILLER WEDGE NO. 1
E55-02232013	1	E55-02232013	FILLER WEDGE NO. 0
E55-02232017	1	E55-02232017	PARALLEL PIN
E55-02232018	1	E55-02232018	FLAT TOP PLATE
E55-02232019	1	E55-02232019	FLAT BACK PLATE
E55-02232021	1	E55-02232021	FILLER PLATE
E55-02232022	1	E55-02232022	NAN-BAR FRAME SIDE TOP
E55-02232023	1	E55-02232023	NAN-BAR FRAME TOP PLATE
E55-02232024	1	E55-02232024	NAN-BAR FRAME BOTTOM PLATE

### SECTION D-D (1:5)

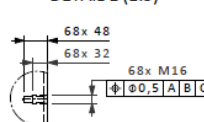
4 PLACES

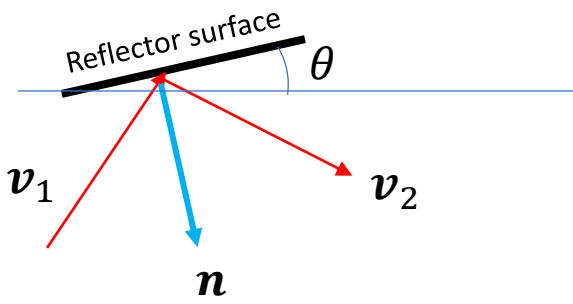


## SECTION C-C



DETAIL E (1·5)





Reflection:

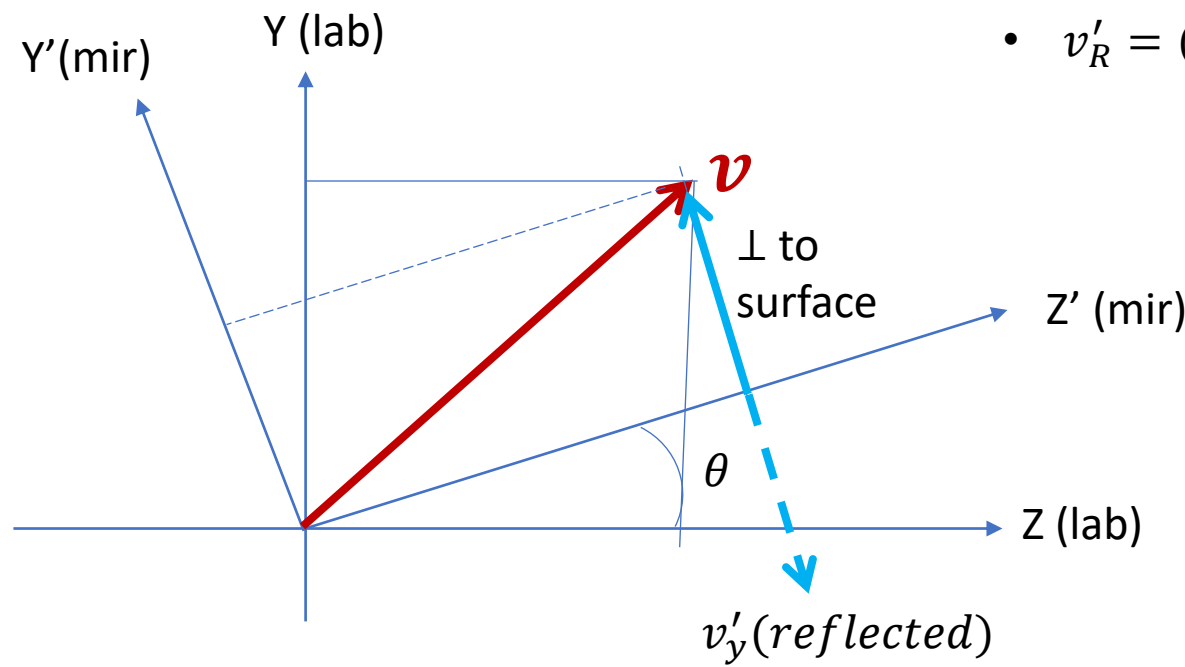
- Mirror is at angle  $\theta$  to horizontal as a rotation around  $\hat{x}$

- $\mathbf{v} = (v_x, v_y, v_z)$

$$\begin{pmatrix} v'_x \\ v'_y \\ v'_z \end{pmatrix} = \begin{pmatrix} 1 & 0 & 0 \\ 0 & \cos\theta & -\sin\theta \\ 0 & \sin\theta & \cos\theta \end{pmatrix} \begin{pmatrix} v_x \\ v_y \\ v_z \end{pmatrix}$$

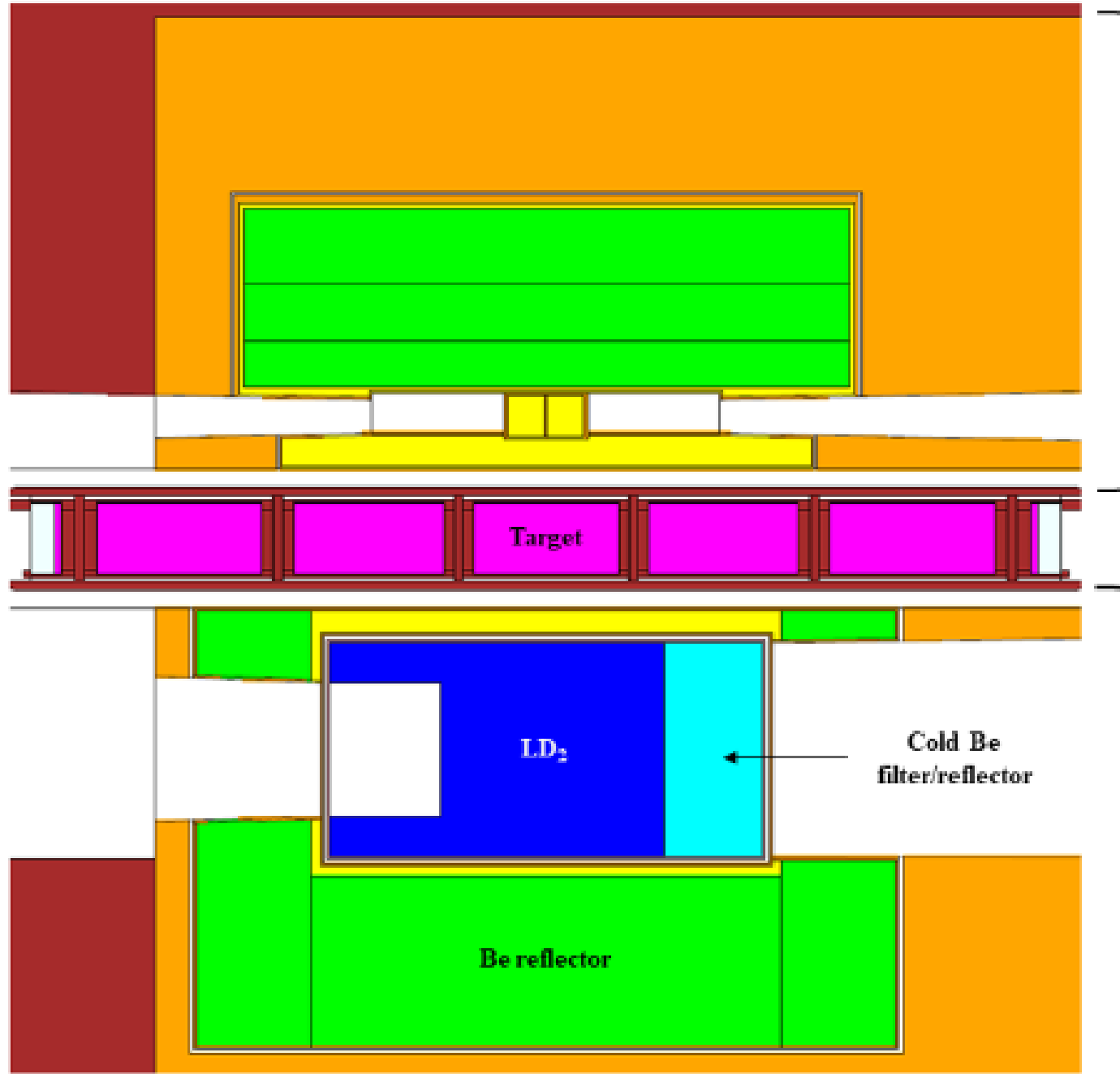
- $v'_R = (v'_x, -v'_y, v'_z)$  vector of reflected neutron

$$\begin{pmatrix} v_x \\ v_y \\ v_z \end{pmatrix} = \begin{pmatrix} 1 & 0 & 0 \\ 0 & \cos\theta & +\sin\theta \\ 0 & -\sin\theta & \cos\theta \end{pmatrix} \begin{pmatrix} v'_x \\ v'_y \\ v'_z \end{pmatrix}$$



Then, the reflected velocity in the lab frame:

$$\begin{pmatrix} v_x \\ v_y \\ v_z \end{pmatrix}^R = \begin{pmatrix} 1 & 0 & 0 \\ 0 & -\cos 2\theta & \sin 2\theta \\ 0 & \sin 2\theta & \cos 2\theta \end{pmatrix} \begin{pmatrix} v'_x \\ v'_y \\ v'_z \end{pmatrix}$$



Upper  
Moderator  
Plug

Lower  
Moderator  
Plug

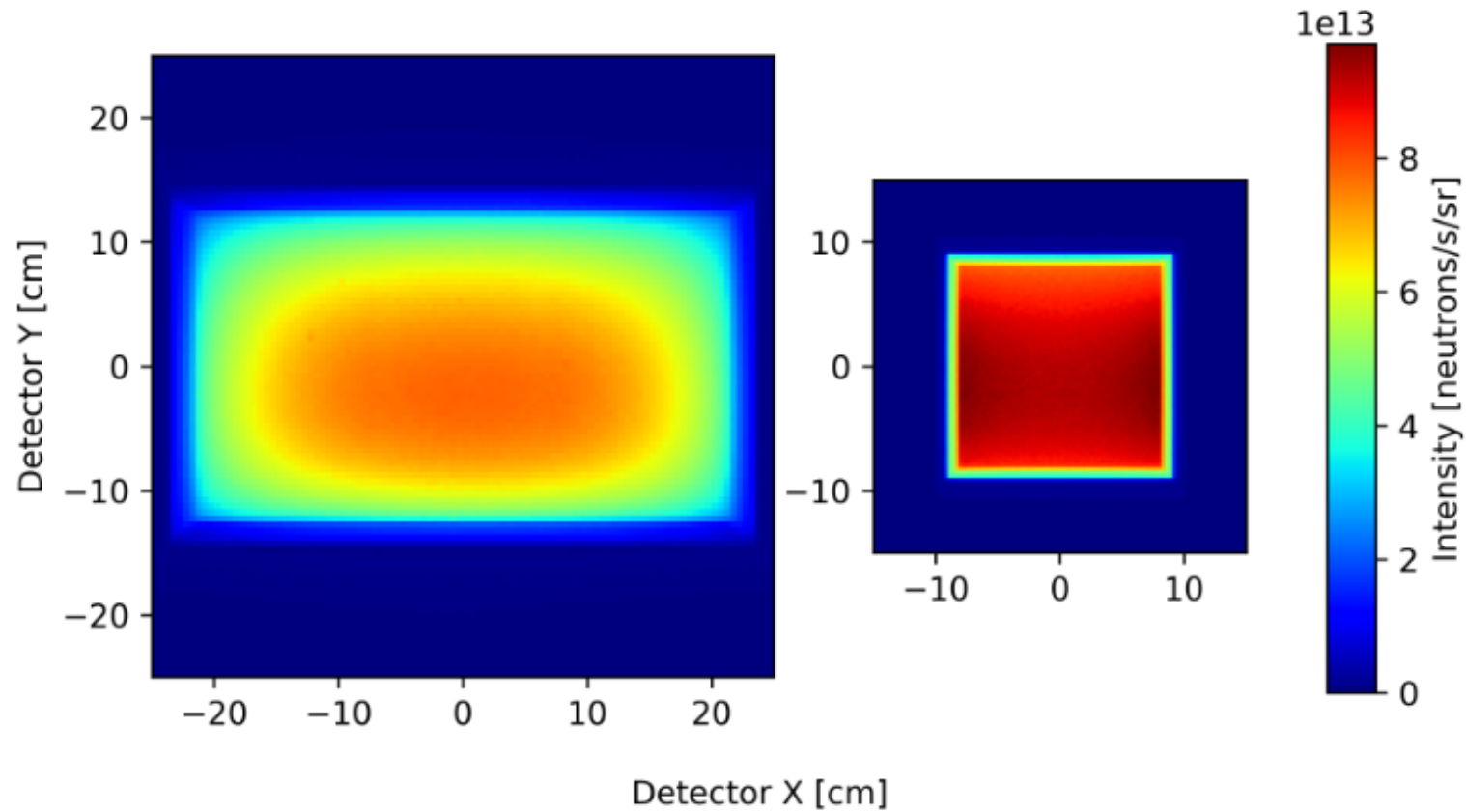
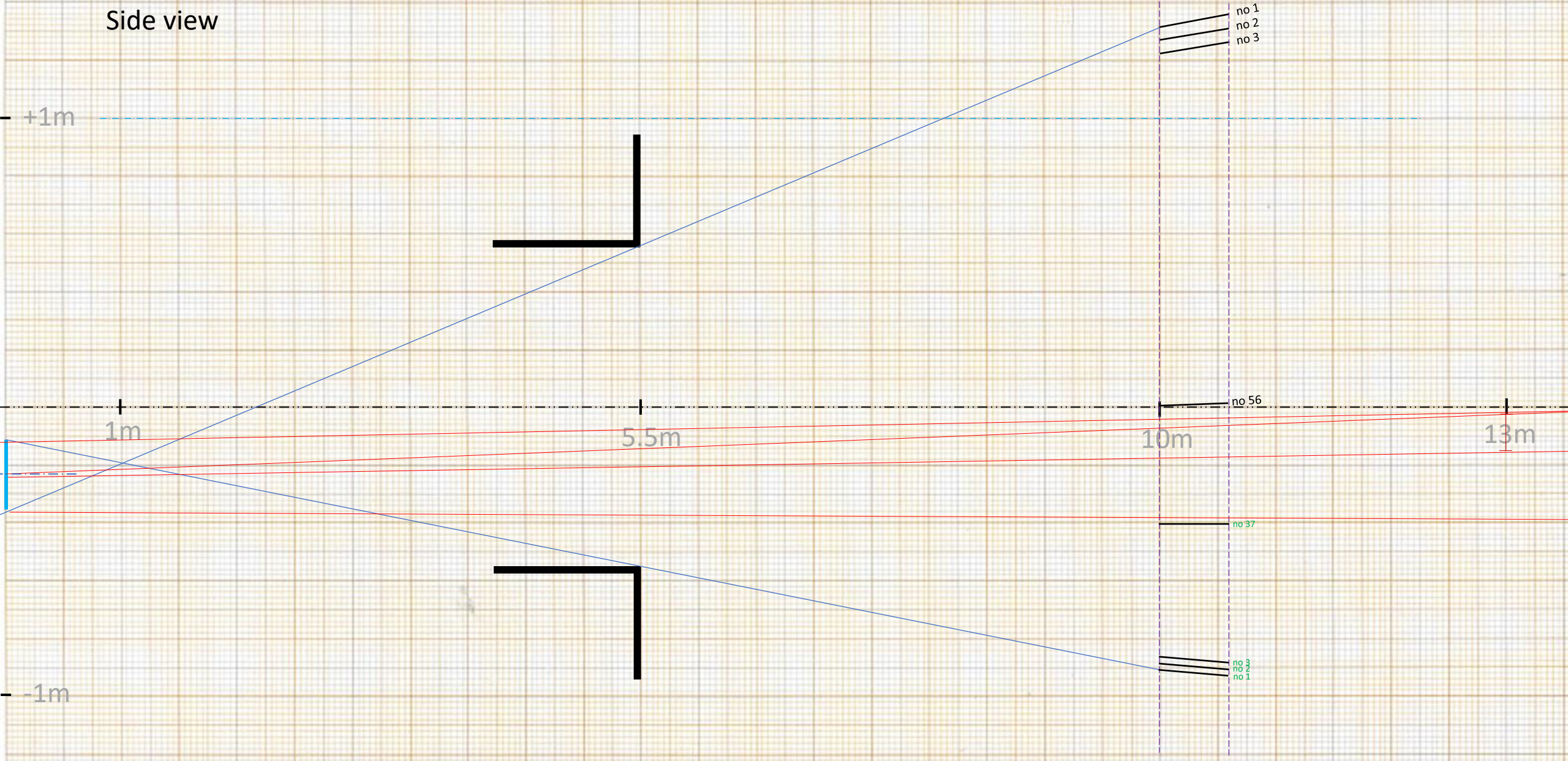
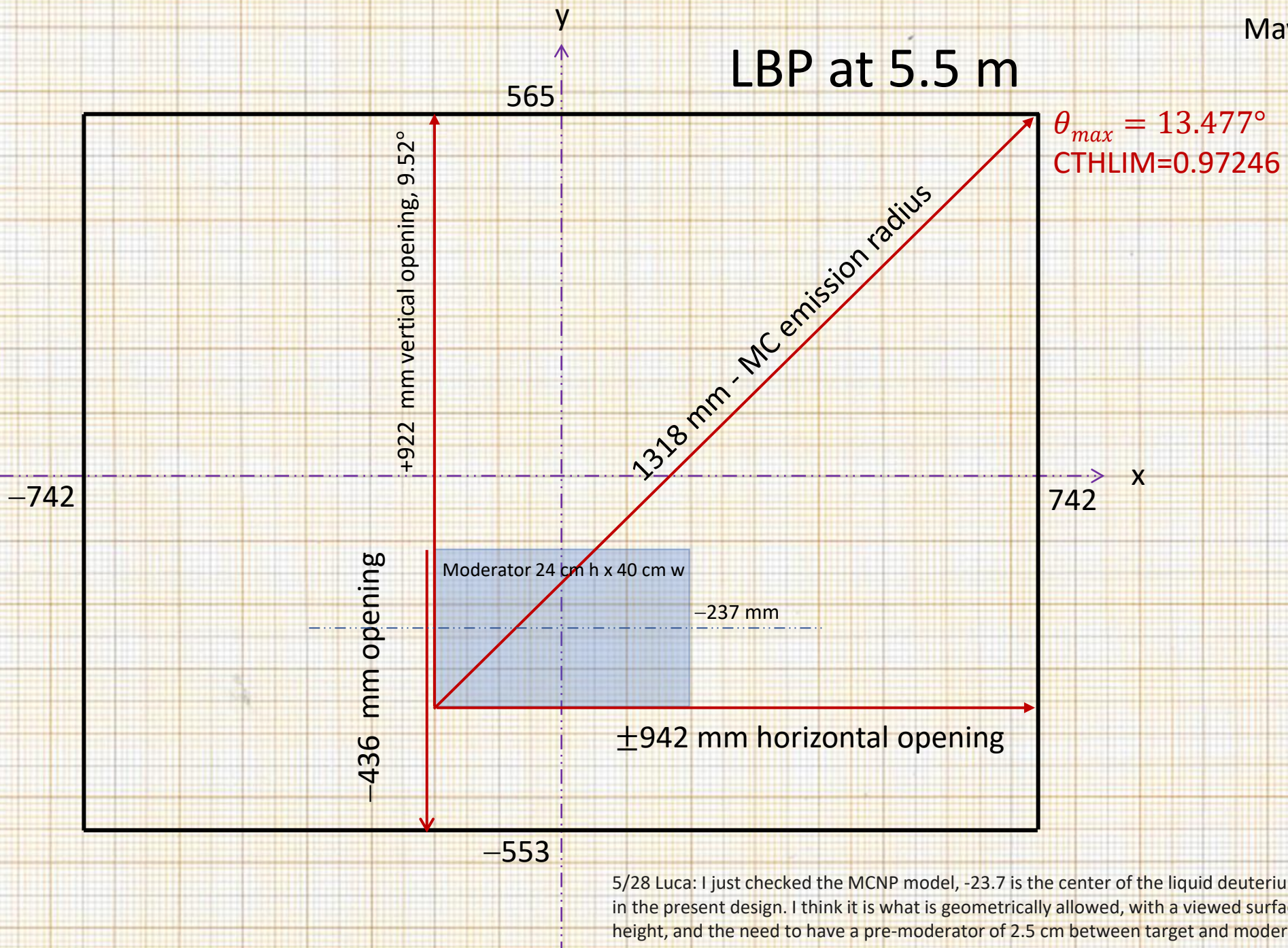


Figure 10: Pinhole images of the  $24\text{ cm} \times 40\text{ cm}$  NNBAR opening (left) and the  $15\text{ cm} \times 15\text{ cm}$  opening for neutron scattering experiments with a filter for cold neutrons ( $\lambda > 4\text{ \AA}$ ). The pinhole is placed at 2 m from the center of the moderator along the central axis, while the detector is 2 m away from the pinhole on the same axis. The pictures are inverted along the vertical direction due to the camera obscura effect.

Side view

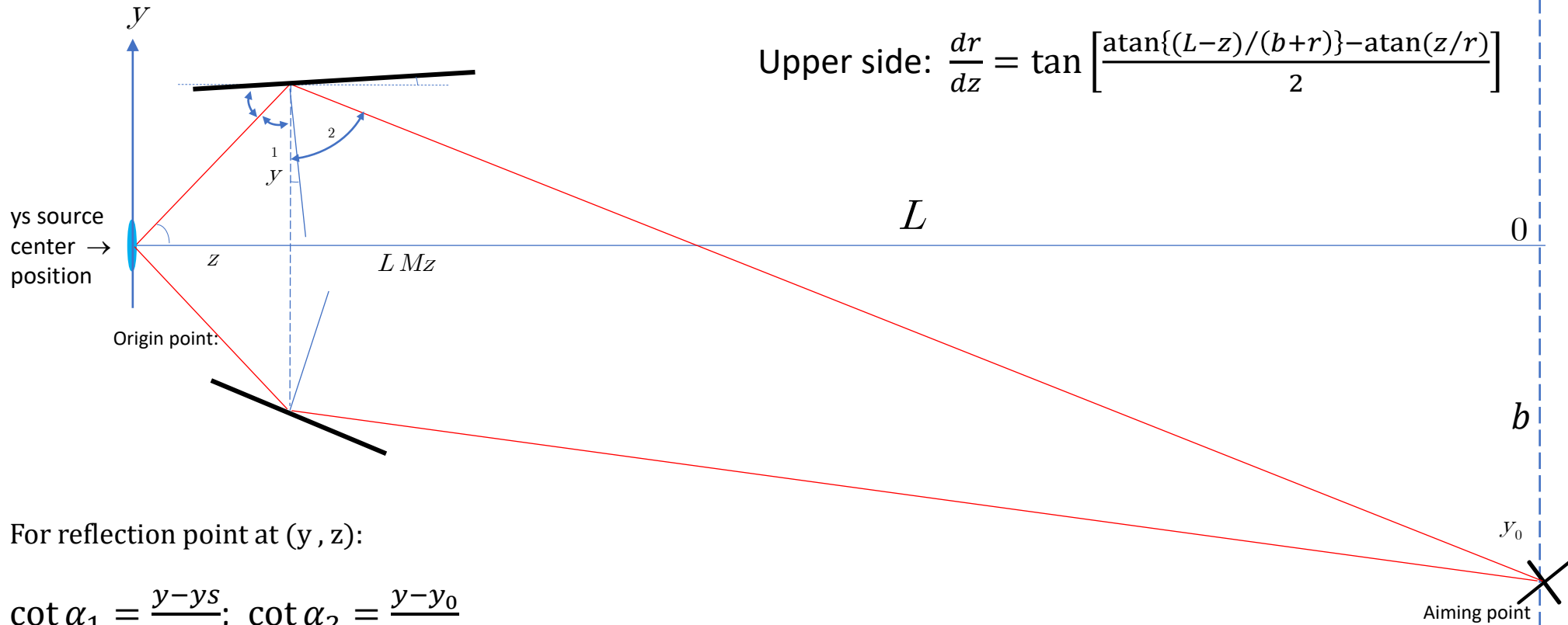






# Reflector geometry

only vertical plane, no gravity



$$\alpha_1 + \beta = \alpha_2 - \beta; \quad \beta = \frac{\alpha_2 - \alpha_1}{2}$$

Upper side:  $\frac{dr}{dz} = \tan \left[ \frac{\text{atan}\{(L-z)/(b+r)\} - \text{atan}(z/r)}{2} \right]$

Lower side:  $\frac{dr}{dz} = \tan \left[ \frac{-\text{atan}\{(L-z)/(b-r)\} - \text{atan}(z/r)}{2} \right]$

```
yposl(200),ystsl(200),delposl(200),blllenl(200),
+yendl(200)
```

common /HREFL/zhr1,zhr3,dzh,nblades,nbladel,dblmin

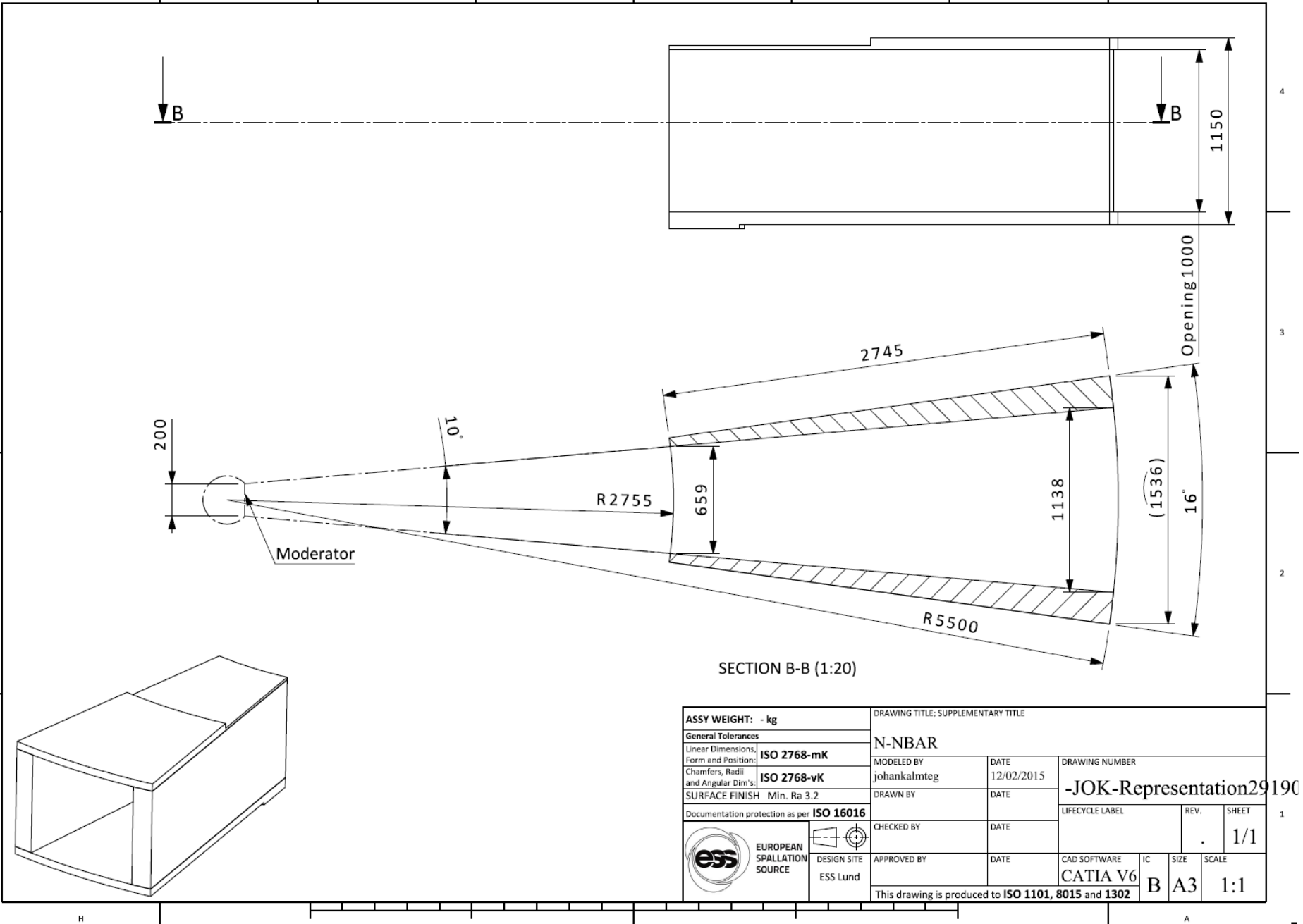
c --> COMMON /PARSOR/

c RSX - moderator half X-size (tot 40 cm)  
c RSY - moderator half Y-size (tot 24 cm)  
c RSH - moderator center position of the source (<0)  
c xmaxLBP - in m +/- x-opening of LBP  
c ymaxLBP - in m + y opening of LBP  
c yminLBP - in m - y opening of LBP  
c zLBP - z-exit of LBP

COMMON

/PARSOR/RSX,RSY,RSH,xmaxLBP,ymaxLBP,yminLBP,zLBP

and /VXB/xsts(200),xpos(200),delpox(200),bllex(200),xend(200)



```
subroutine hblade(zs,zhr,zhr1,dzh,yst,ys,ztarp,ytarp,yrc,delta)
c -----
c horizontal blade position&angle calculation
c blade starts at given points (yst,zhr1) in projectio
c and angle delta to horizontal is calculated for straight
c trajectories coming from the center of moderator
c --> input: zs,ys - z and y position of source center
c --> input: zhr - z position of the center of refl. package
c --> input: dzh - half z-extension of reflector package
c --> input: zhr1 - z-beginning of reflection pachage
c --> input: ztarp and ytarp z and y position of annih. target center
c --> output:yst,yrc,delta beginning,center, and angle of the blade n
c
c----For initial starting point yst at zhr1 solves equations with two unknowns
c----yrc - center of blade at position zhr in vertical projection and
c----delta - angle in radians of the blade slope (dy/dz derivative)
c --> zhr(e.g.)=10.0 ! z position of centers of horizontal blades
c
c --> first, let's start with initial delta (if center of the blade yrc
c --> would be equal to yst at position zhr1
```

```
common /NSOUR/XS0,YS0,ZS0,XDC,YDC,ZDC,VEL,NSGEN
common /HREFL/zhr1,zhr3,dzh,nblades,nbladel,nbladex,dblmin
common /HVB/ysts(200),ypos(200),delpo(200),bllen(200),yend(200)
common /HVL/ytsl(200),yposl(200),delposl(200),bllenl(200),yendl(200)
common /VXB/xsts(200),xpos(200),delpox(200),bllex(200),xend(200)
common /TARGET/xtarp,ytarp,ztarp,rtarg
COMMON /PARSOR/RSX,RSY,RSH,xmaxLBP,ymaxLBP,yminLBP,zLBP
```

X-Y distribution at z=200 m for  
point-like source (0,-0.237,0)  
with gravity g = 0

HBOOK ID = 120 DATE 07/06/2022 NO = 20  
 CHANNELS 100 U 0 1 0  
 10 N 0 1 2 3 4 5 6 7 8 9 0 V  
 1 D 123456789012345678901234567890123456789012345678901234567890123456789012345678901234567890 E  
 \*\*\*\*\*  
 OVE \* + \* OVE  
 2.85 \* \* 50  
 2.7 \* \* 49  
 2.55 \* \* 48  
 2.4 \* \* 47  
 2.25 \* \* 46  
 2.1 \* \* 45  
 1.95 \* \* 44  
 1.8 \* \* 43  
 1.65 \* \* 42  
 1.5 \* \* 41  
 1.35 \* \* 40  
 1.2 \* \* 39  
 1.05 \* \* 38  
 .9 \* \* 37  
 .75 \* \* 36  
 .6 \* \* 35  
 .45 \* \* 34  
 .3 \* \* 33  
 .15 \* \* 32  
 \* \* 95F29C4H8B ABB538876987478DH78BB387A545762588\*\*\*\*\*+757675768477B365A4584A7CD66A46847 9C769A3F45 \* \* 32  
 \* \* J4P96097CK AF7A6C77CCDA97CEH87DB2H7EC827646B7\*\*\*\*\*+85775A9589613FB69E667E97GFA6A2CFB75BDC6GE9J59 \* \* 31  
 - .15 \* \* 30  
 \* \* A4F68CGE1G2ECB736EB7ICA8AFAE98AAB93EA68895989\*\*\*\*\*+249A5897CA5G9A77CH7A8D9F78FE69LH951F47J54K59 \* \* 30  
 - .3 \* \* 29  
 \* \* CAF3GD3+CB CIJ93ABD86998968267+A672763357235\*\*\*\*\*+342594569 75B39EA7D45A479B5B225AB A964I82A46 \* \* 29  
 - .45 \* \* 28  
 \* \* 435 76 644 273++34543963+++4632926+332 23 2+\*\*\*\*\* 4+2 62235 5233 32 22233634+55444+ 334 66 3++ \* \* 28  
 - .6 \* \* 27  
 - .75 \* \* 26  
 - .9 \* \* 25  
 - 1.05 \* \* 24  
 - 1.2 \* \* 23  
 - 1.35 \* \* 22  
 - 1.5 \* \* 21  
 - 1.65 \* \* 20  
 - 1.8 \* \* 19  
 - 1.95 \* \* 18  
 - 2.1 \* \* 17  
 - 2.25 \* \* 16  
 - 2.4 \* \* 15  
 - 2.55 \* \* 14  
 - 2.7 \* \* 13  
 - 2.85 \* \* 12  
 - 3 \* \* 11  
 - 3.15 \* \* 10  
 - 3.3 \* \* 9  
 - 3.45 \* \* 8  
 - 3.6 \* \* 7  
 - 3.75 \* \* 6  
 - 3.9 \* \* 5  
 - 4.05 \* \* 4  
 - 4.2 \* \* 3  
 - 4.35 \* \* 2  
 - 4.5 \* \* 1  
 UND \* \* UND

## ESS LBP spectrum on target with/without gravity

$$g = 9.8$$

| g = 0.0

```

*          1366.08 I 2026II 1369.404
* ENTRIES = 77527 PLOT -----I-----I-----
* SATURATION AT= INFINITY 3409.062I 88976I 3429.784
* SCALE .+,2,3,...,A,B, STATISTICS -----I-----I-----
* STEP = 1.00 * MTNMINM=0.00 276 206I 5387.429I 320.762

```

LOW-EDGE -----  
10 1

```

*      0     08642086420864208642086420864208642086420864202468024680246
* ENTRIES = 4219          PLOT      1390_0411   16471_1386_989
* SATURATION AT= INFINITY
* SCALE +,-2,3,...,A,B, STATISTICS 1696_8831 44221_1742_431
* STEP = 1.00,...,* MINIMUM=0.00 204_72_1 2315_54_51 256_02_0

```

2 MW, LBP LD2 source,  
gravity ON, m=6 reflector  
Target displacement -1.5 m

W-EDGE

1

2 MW, LBP LD2 source, gravity ON, m=6 reflector, target displacement -1.5 m

## X-Y on target plane with N=weight

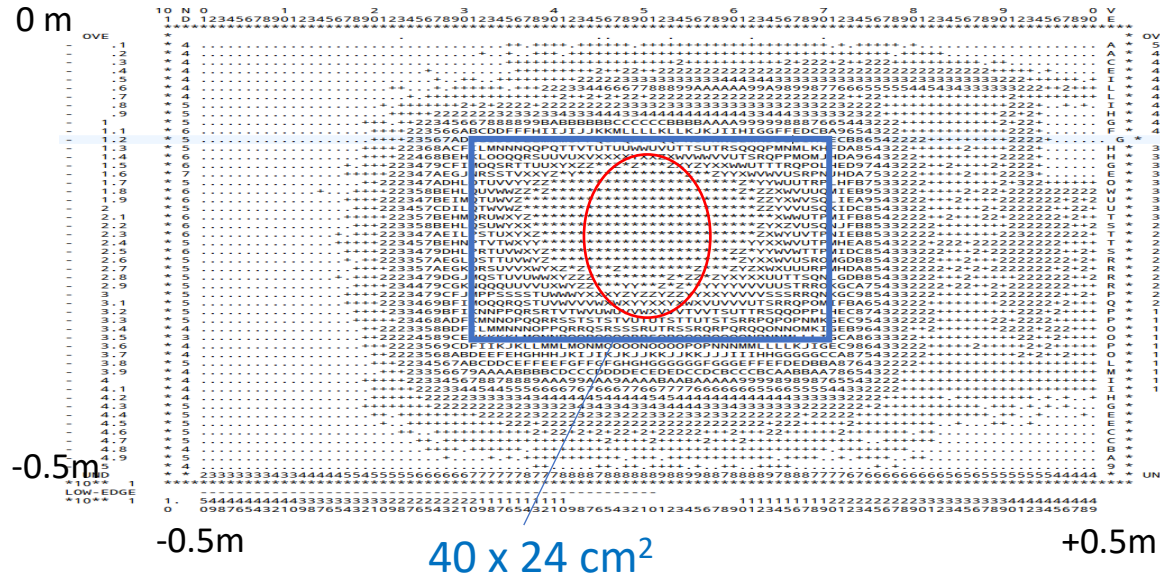
X-Y on target plane with  $N^*t^2$ =weight



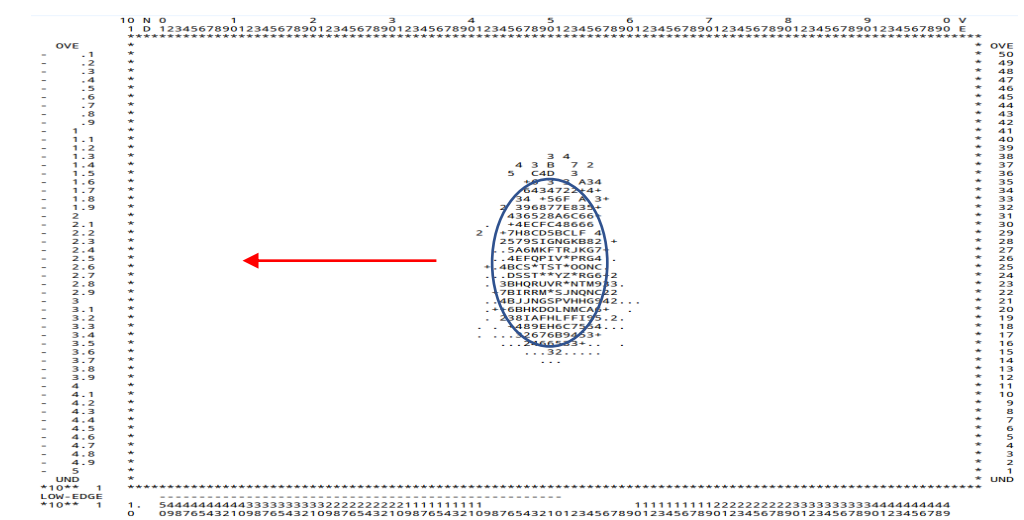
# Target hits select only small area of the source.

## Not all area of the source is efficient for creating $Nt^2$

Neutrons that reached the target plane  $z = 200$  m were originated in the source plane as ↓



Back image of the target with dia 2 m in the source plane through the V-B reflector



## Matt Frost sensitivity calculations with large LD2 moderator and differential reflector

Matt Frost/ORNL sensitivity calculation (comparison with Richard's simulations)

Event file provided by Richard Wagner on June 3, 2022, with LBP opening  $\pm 5^\circ$  and LD2 moderator  $40 \times 24 \text{ cm}^2$  centered at  $Y=23.7 \text{ cm}$  from ESS axis

Differential reflector configuration from 10 to 50 m with  $m=6$

Source-Detector L=200 m, target radius 1m, detector efficiency = 50%  
(plots on the next page)

Normalization integral in this calculations: 1 ILL unit =  $1.8\text{E}+9 \text{ n} \cdot \text{s}$

In Matt's thesis normalization integral: 1 ILL unit =  $2.0\text{E}+9 \text{ n} \cdot \text{s}$

07/31/2022 calculation [119. ILL/yr/MW](#) with 1 ILL unit =  $2.0\text{E}+9 \text{ n} \cdot \text{s}$  with ESS  $40 \times 24 \text{ cm}^2$  event file  
133. ILL/yr/MW with 1 ILL unit =  $1.8\text{E}+9 \text{ n} \cdot \text{s}$  with ESS  $40 \times 24 \text{ cm}^2$  event file

MJF thesis with 1 ILL =  $2.0\text{E}+9 \text{ n} \cdot \text{s}$  66.6 ILL/yr/MW (with old Esben's spectrum)  
if 1 ILL =  $1.8\text{E}+9 \text{ n} \cdot \text{s}$  74 ILL/yr/MW (with old Esben's spectrum)

---

Richard's calculations with Esben's file (?) FOM=58.0 ILL/yr/MW (1 ILL unit =  $2.0\text{E}+9 \text{ n} \cdot \text{s}$ ?)

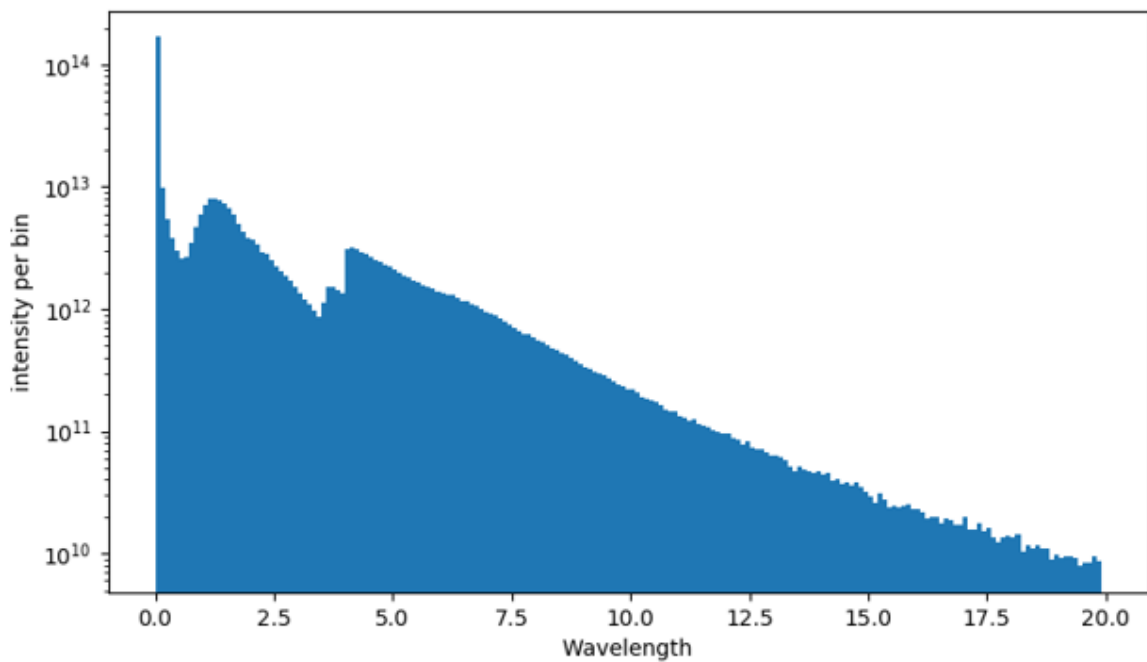
Richard's calculations with June 3, 2022, ESS event file [FOM=93.6 ILL/yr/MW](#) (1 ILL unit =  $2.0\text{E}+9 \text{ n} \cdot \text{s}$ ?)

# Matt's notes from 07/31/2022 simulation producing FOM=133 ILL/yr/MW

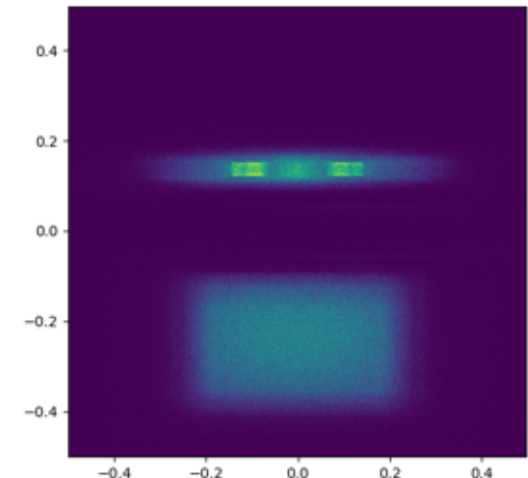
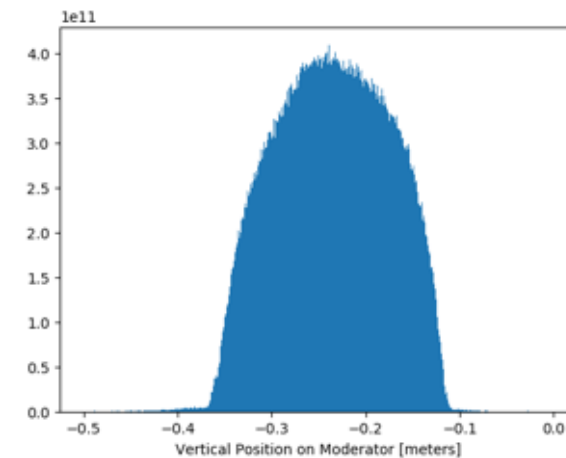
## New NNbar Notes

Weights need to be multiplied by 1.56e16 for 5MW operation, I've set this to be per MW.

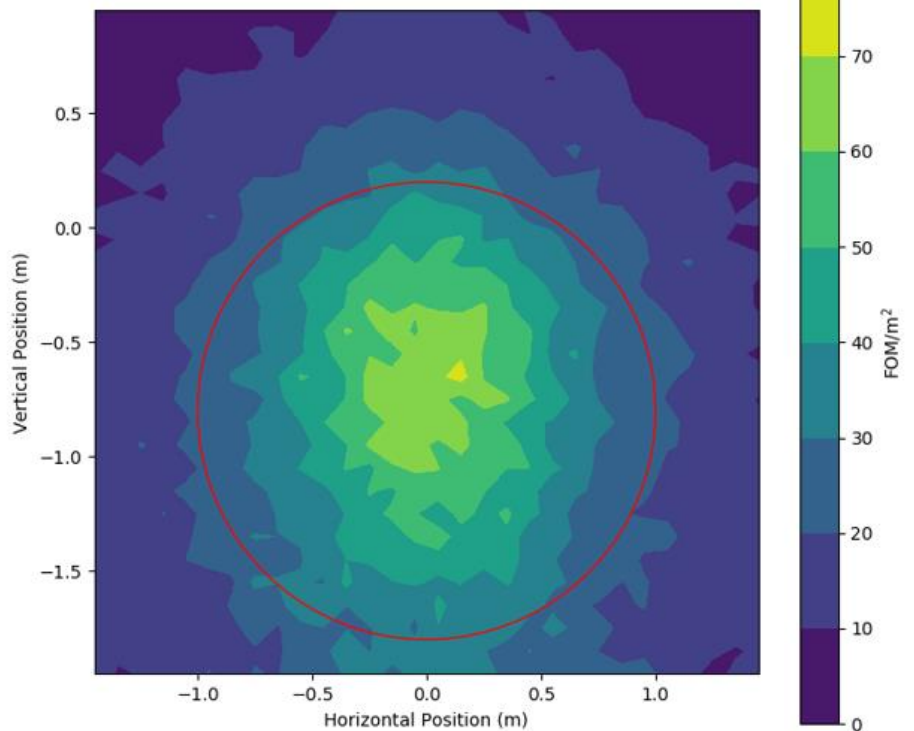
Lower moderator assumed to be centered at -237 mm below proton beam axis.



Able to convert velocity to wavelength, assume cuts are due to Beryllium filter. Substantial amount of high energy events. Will start at 0.1 Angstrom for sensitivity analysis, suggest use of same hard spectrum for background analysis. Cut sets events number to 2.82e6, down from 4.35e6. x and y origin view with that cut. Clearly, the only events of interest are in the lower area. A filter was taken below 1000 m/s to see where the most intense location is on the moderator face.



07/31/2022 FOM=133 ILL/yr/MW Matt Frost/ORNL



No re-optimization of the focal point; the same geometry used in MJF thesis. Using  $1.8\text{e}9 \text{ n-s per yr/ILL}$  and 50% detector efficiency, I find 131 ILL units per year per MW of beam power. More optimization of the reflector can be performed, but this is a significant improvement over my original 333 ILL/yr at 5 MW with  $2.0\text{e}9 \text{ n-s per yr/ILL}$ .



## Matt Frost/ORNL sensitivity calculation (comparison with Venetian Blinds reflector)

Event file provided by Richard Wagner on June 3, 2022, with LBP opening  $\pm 5^\circ$  and LD2 moderator 40 x 24 cm<sup>2</sup> centered at Y=23.7 cm from ESS axis

Differential reflector configuration from 10 to 50 m with m=6

Source-Detector L=200 m, target radius 1m, detector efficiency = 50%

Normalization integral: 1 ILL unit is 1.8E+9 n · s

07/31/2022 calculation 133 ILL/yr/MW

08/22/2022 calculated in above configuration but **with point-like source** (resetting events in file to x=0, y=-23 cm)

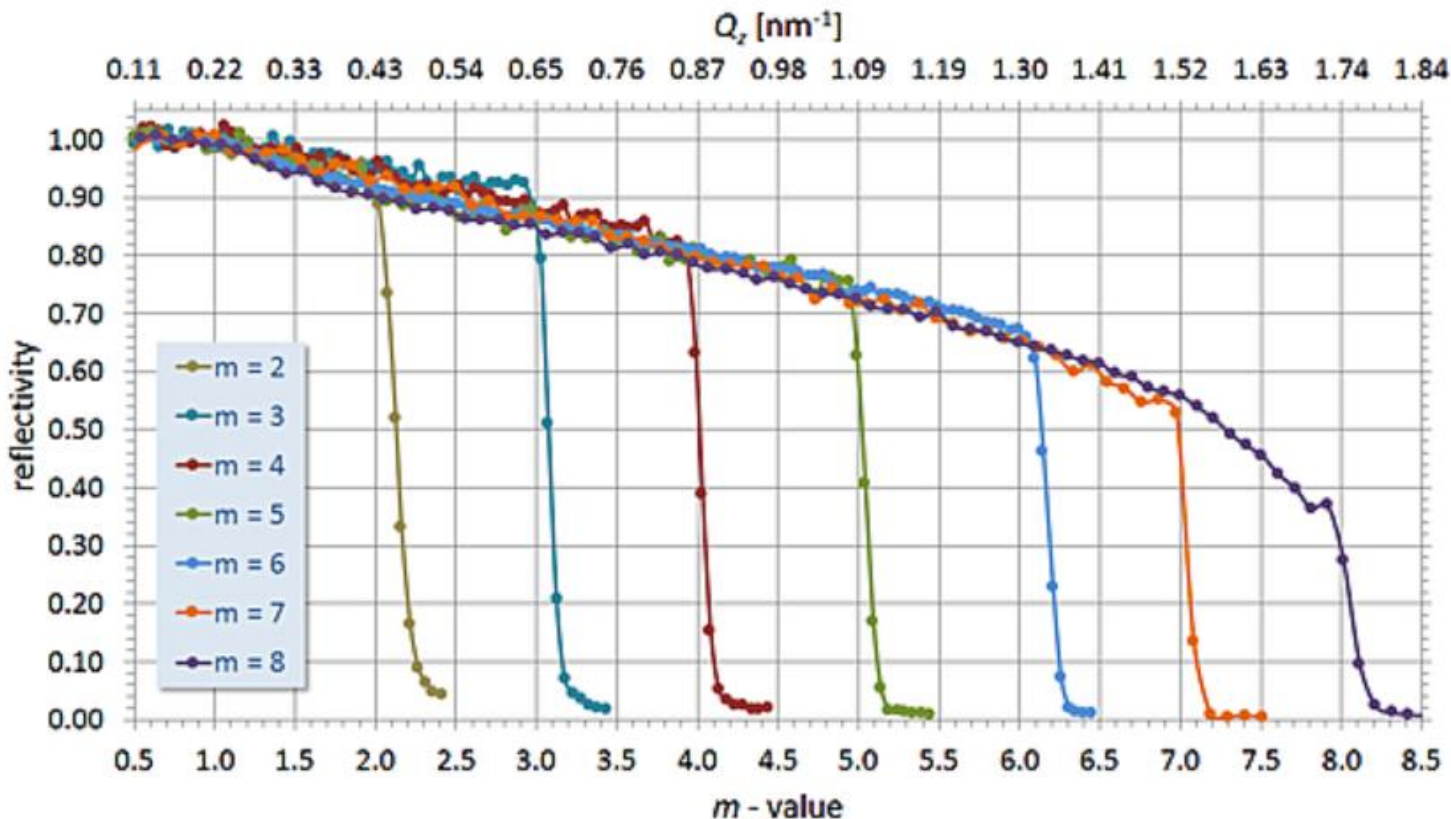
Without gravity 524 ILL/yr/MW MJF thesis with 1 ILL

With gravity ON 278 ILL/yr/MW

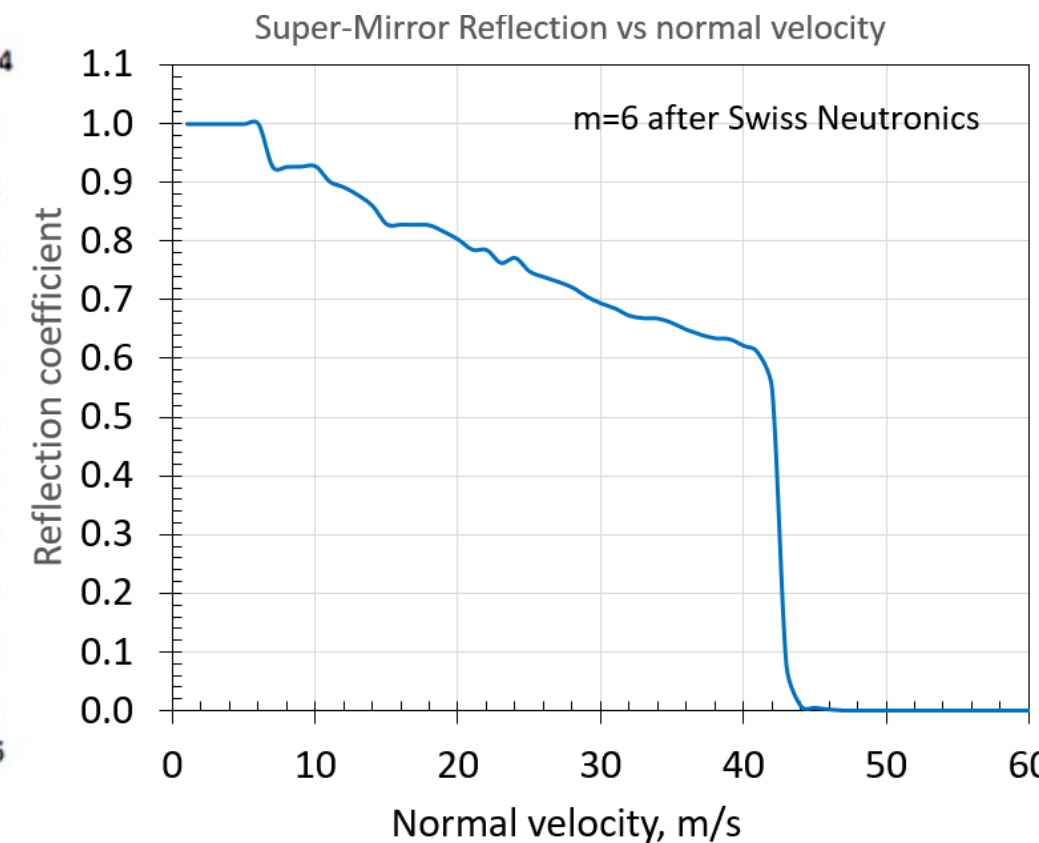
Venetian blinds reflector without gravity



## Ni / Ti & non-depolarising supermirrors



Reflectivity profiles of Ni/Ti & non-depolarising supermirror coatings  $2 \leq m \leq 8$ .



# ESS

<https://arxiv.org/pdf/2211.10396.pdf>

Particle Physics at the European Spallation Source

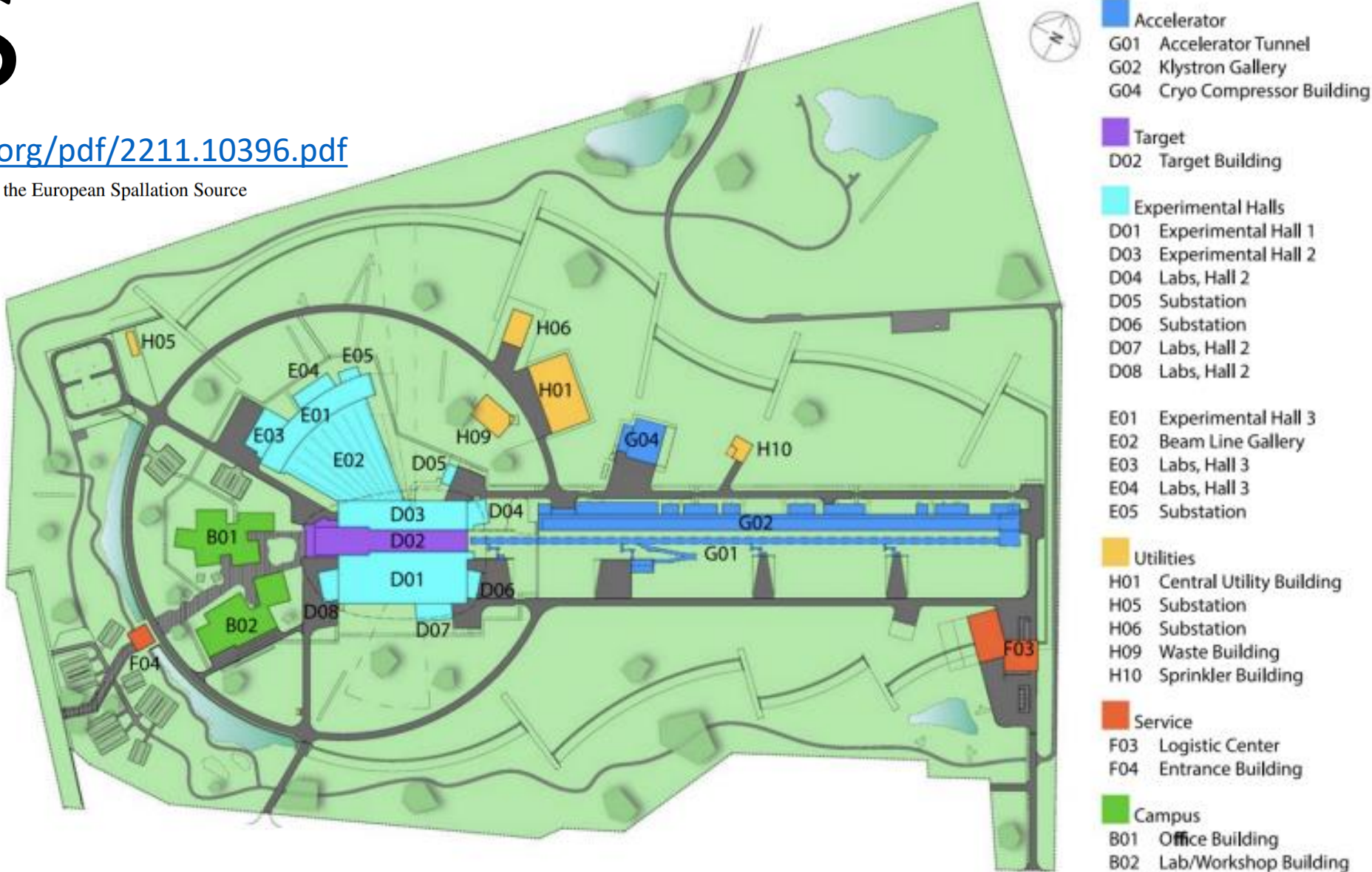


Figure 1: Layout of the ESS infrastructure.

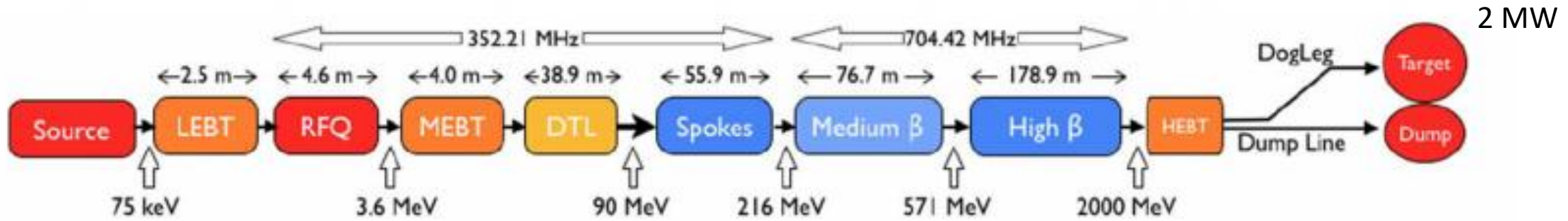


Figure 2: They layout of the ESS linac.

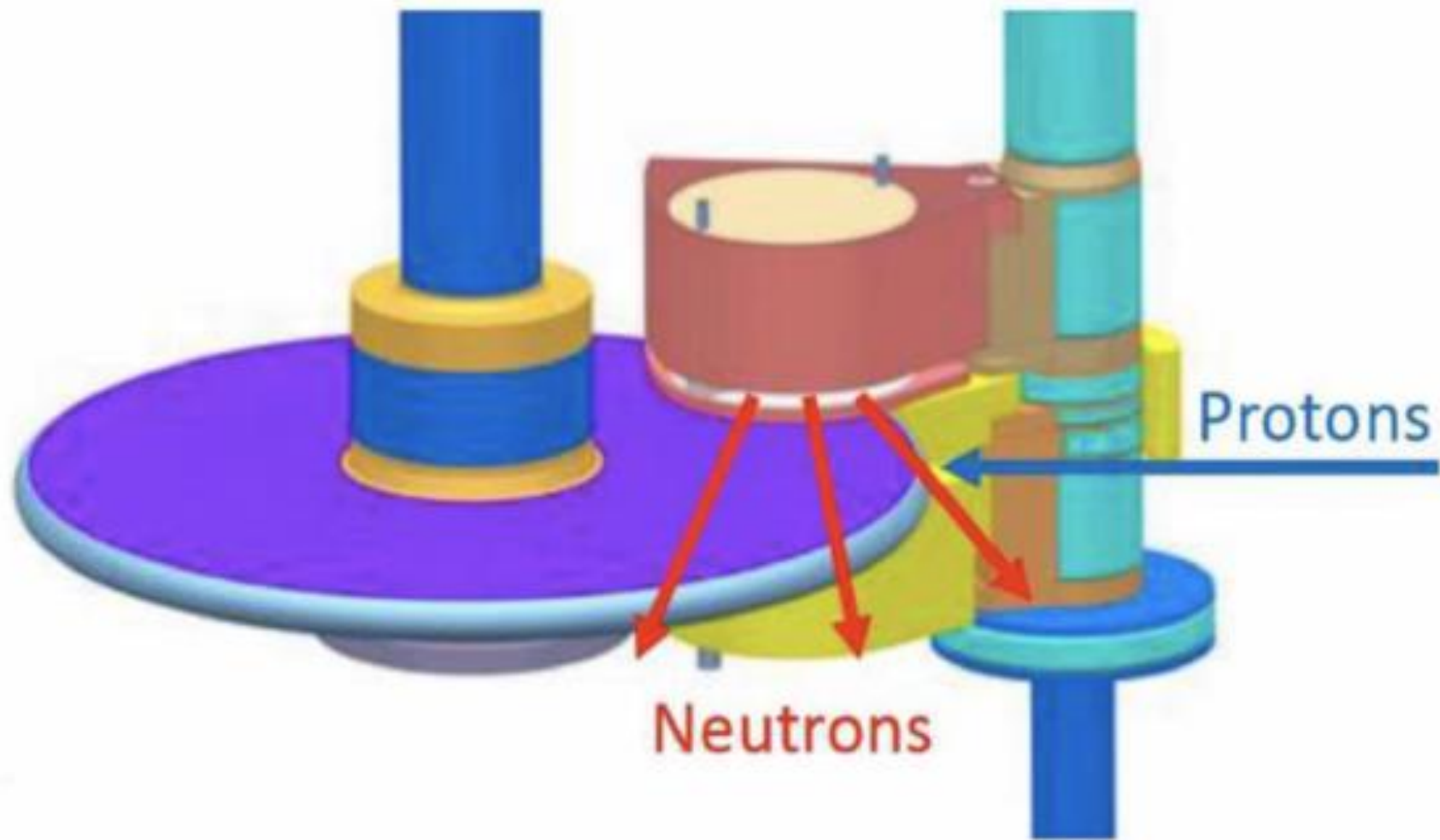
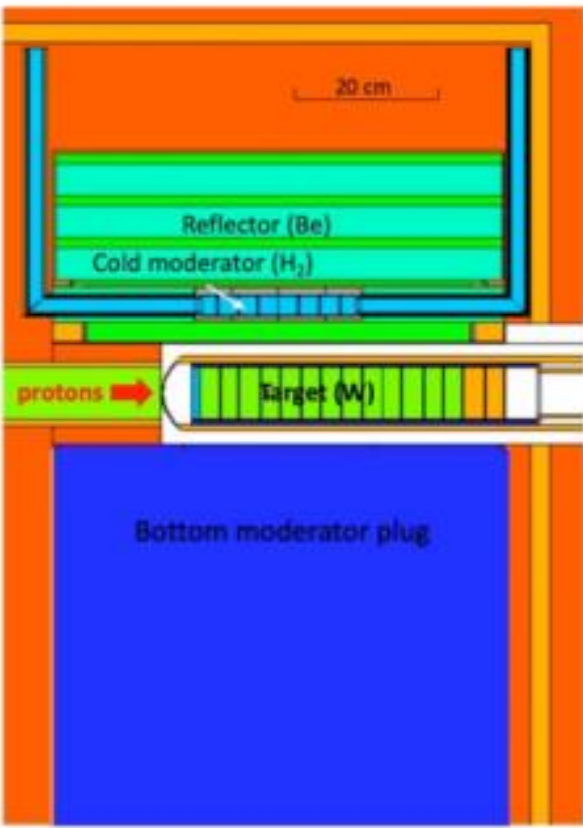


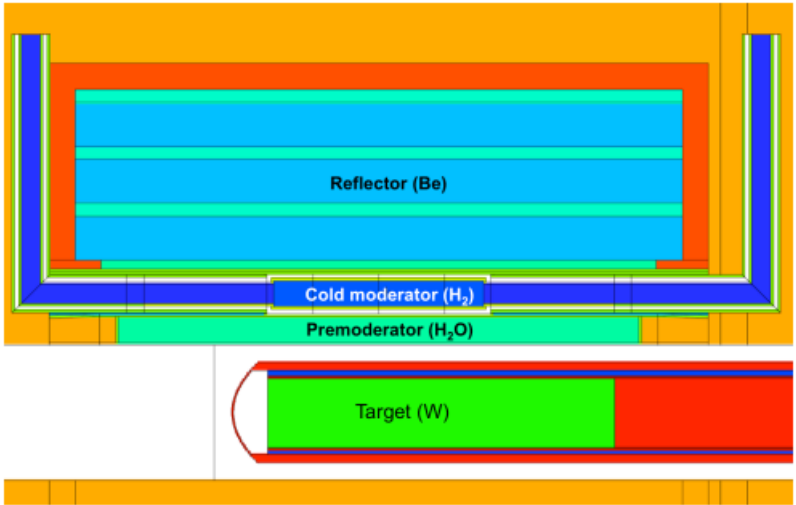
Figure 3: Overview of the ESS target area.



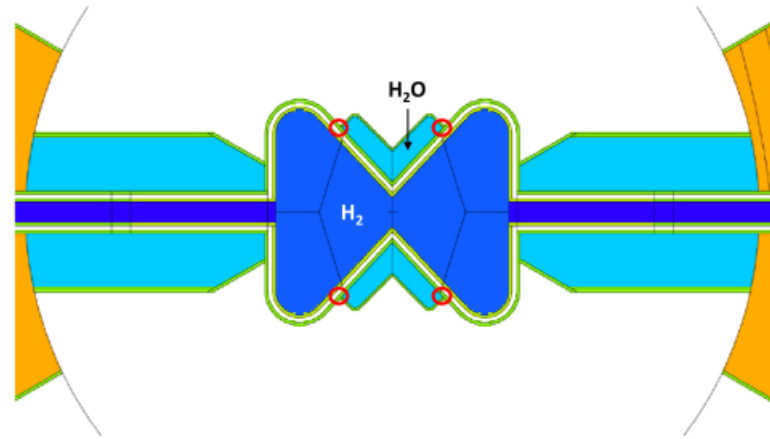
3 cm thickness of moderator



Figure 4: Overview of the ESS upper moderator. Left: MCNP model of the ESS target area in its initial configuration with only a moderator located about the spallation target. Right: Top view of the butterfly moderator. The dark blue represents para hydrogen, while the light blue is water.



**Figure 1.** MCNPX [9] geometry, side view. Proton beam comes from the left impinging on the tungsten target. Tungsten (green) has a density of  $15.1 \text{ g/cm}^3$  instead of the nominal density of  $19.3 \text{ g/cm}^3$  to account for the fraction of helium coolant in the target according to which the filling factor of tungsten is 78 vol%. The beryllium reflector (light blue) includes water channels (green) according to engineering drawings. The reflector is contained in stainless steel (red). The outer reflector (orange) is made of stainless steel, with 10% volume fraction of water, for cooling



**Figure 2.** MCNPX geometry of the moderator, top view. The parahydrogen (blue) contains 5 vol% of Al in the model, to account for the presence of Al flow channels, not yet designed. On the sides of the cold moderator, inlet and outlet hydrogen pipes, including vacuum gaps, are modelled. Water (light blue) is placed around the pipes to serve as premoderator and increase the brightness of the cold moderator. Externally, part of the outer reflector (orange) is shown. The four focal points (origin of the beam ports) are circled in red.

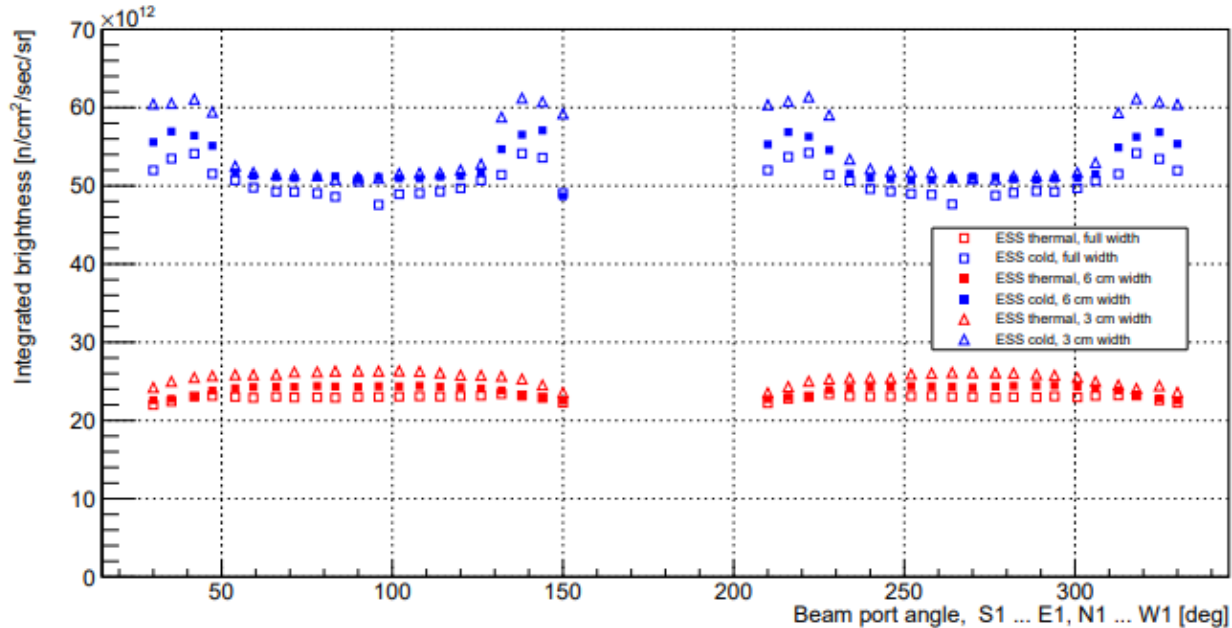


**Figure 3.** Time-average integrated thermal ( $20 < E < 100$  meV) and cold ( $E < 20$  meV) brightness for the 42 beam ports, for different horizontal projected widths: full, 6 cm and 3 cm.

30 times the average ILL brightness [1]. With the use of low-dimensional moderators, we are far above this goal. The cold brightness shown in the present design is (at 4 Å) nearly 140 times higher than the yellow book value. The thermal brightness at 1.5 Å is about 10 times higher than ILL. Considering integral values, the integrated peak cold brightness above 4 Å for the butterfly is of  $4.2 \times 10^{14}$  n/cm<sup>2</sup>/s/sr, which is 125 times the ILL average integrated brightness ( $3.3 \times 10^{12}$  n/cm<sup>2</sup>/s/sr). For the cold neutrons between 2 Å and 4 Å, the ESS brightness is of  $9.1 \times 10^{14}$  n/cm<sup>2</sup>/s/sr, which is 200 times the ILL brightness ( $4.5 \times 10^{12}$  n/cm<sup>2</sup>/s/sr) in the same range. For thermal neutrons, from 0.9 Å to 2 Å, the ESS peak thermal brightness is of  $6.0 \times 10^{14}$  n/cm<sup>2</sup>/s/sr which is about 10 times higher than ILL ( $6.2 \times 10^{13}$  n/cm<sup>2</sup>/s/sr).

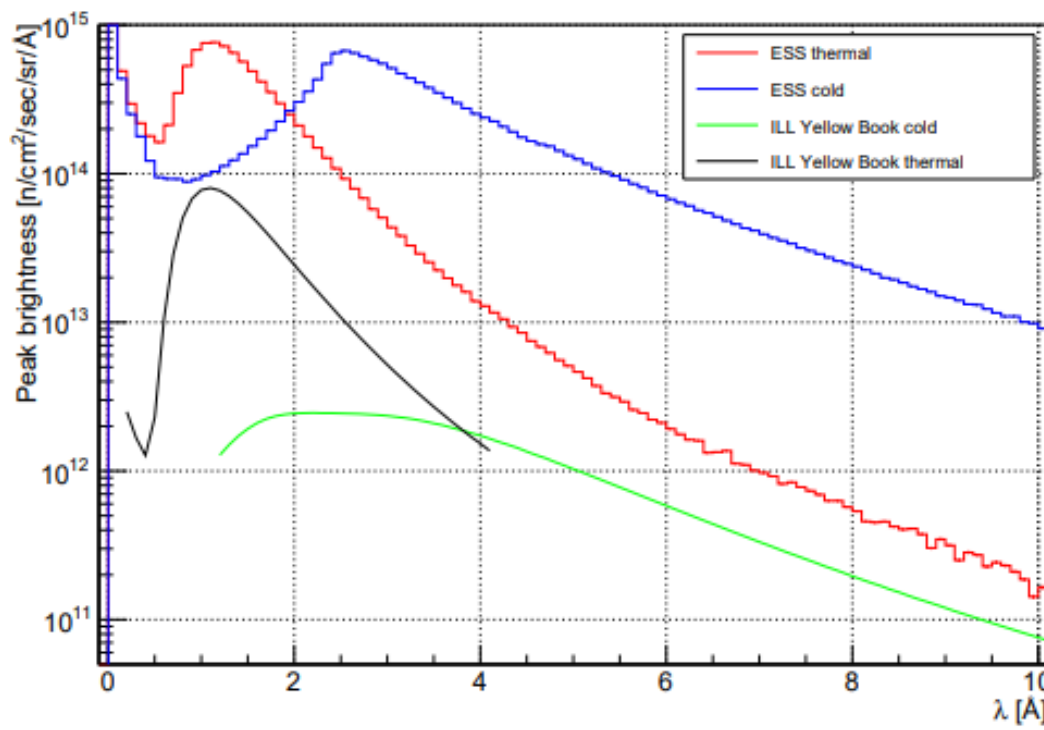


**Figure 4.** Brightness spectra averaged over 42 beam ports for 3 cm high moderator, compared with ILL official curves [8].

<https://arxiv.org/pdf/2211.10396.pdf>

Wall thickness from  $r=11.5$  m to  $r=15.0$  m



Figure 5: The ESS bunker wall.

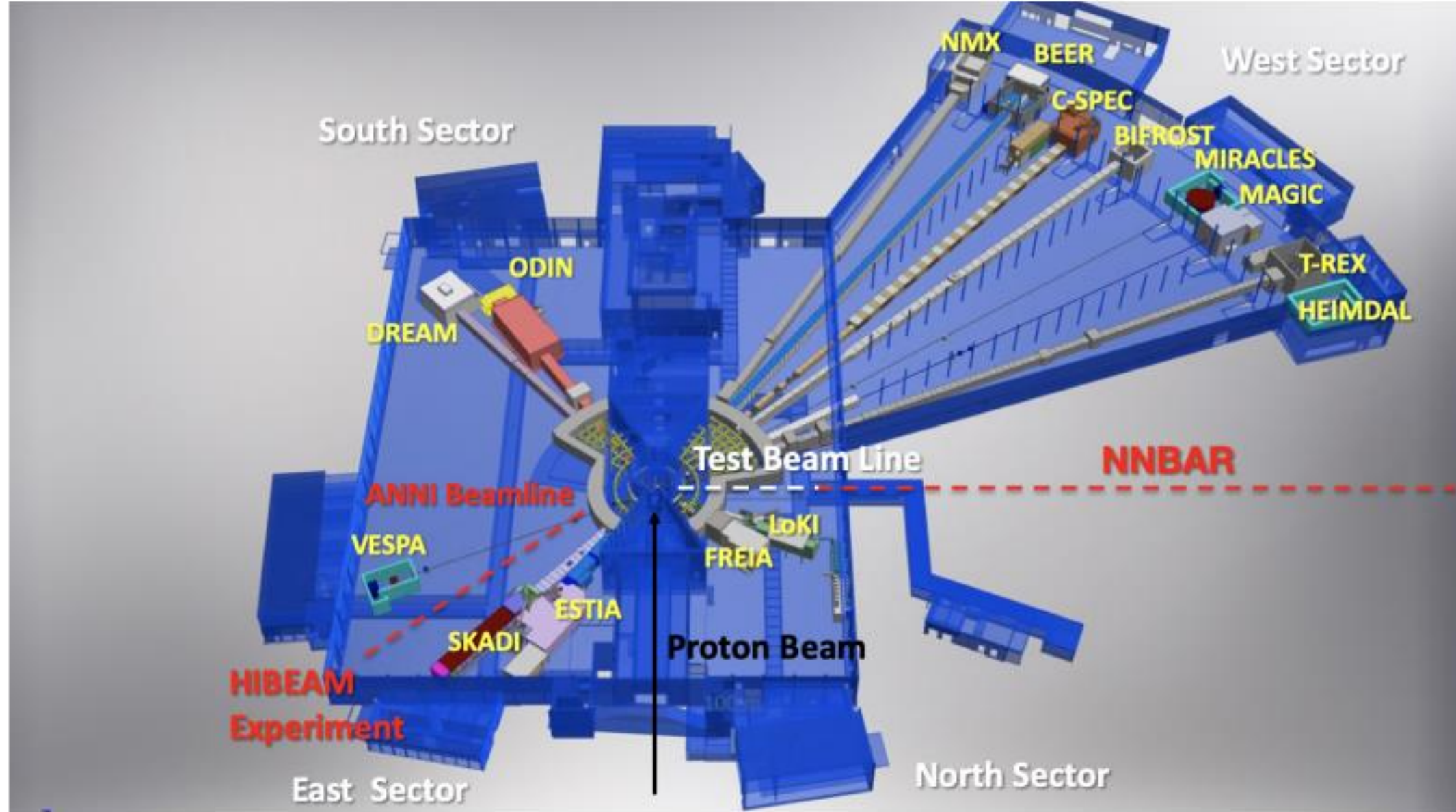


Figure 6: The ESS instrument layout.

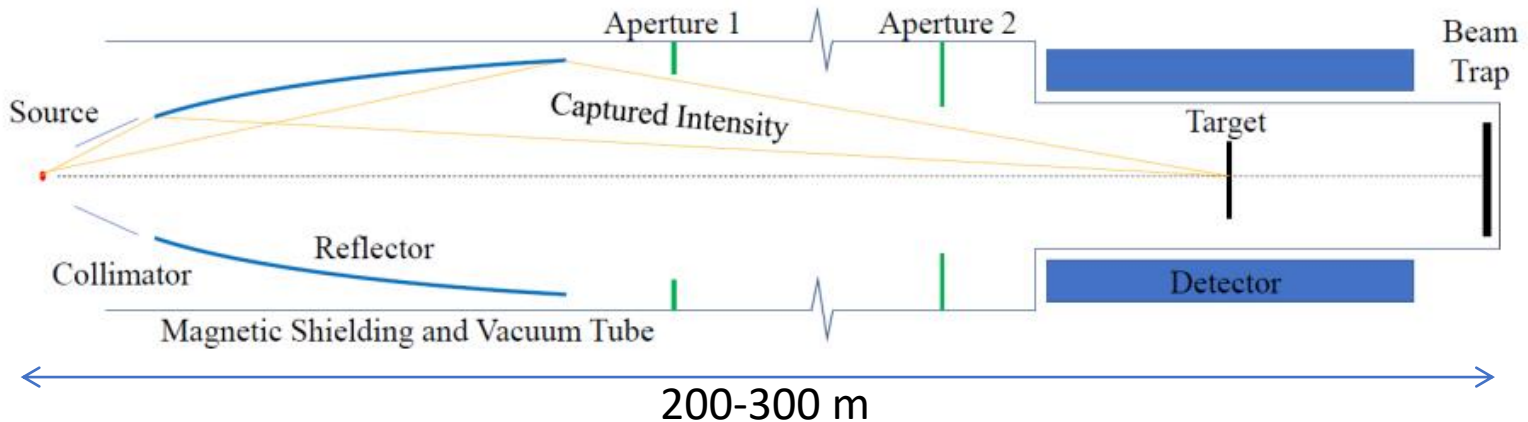


Figure 18: Baseline NNBAR experiment. Neutrons from the moderator are focused on a distant target foil surrounded by an annihilation detector.

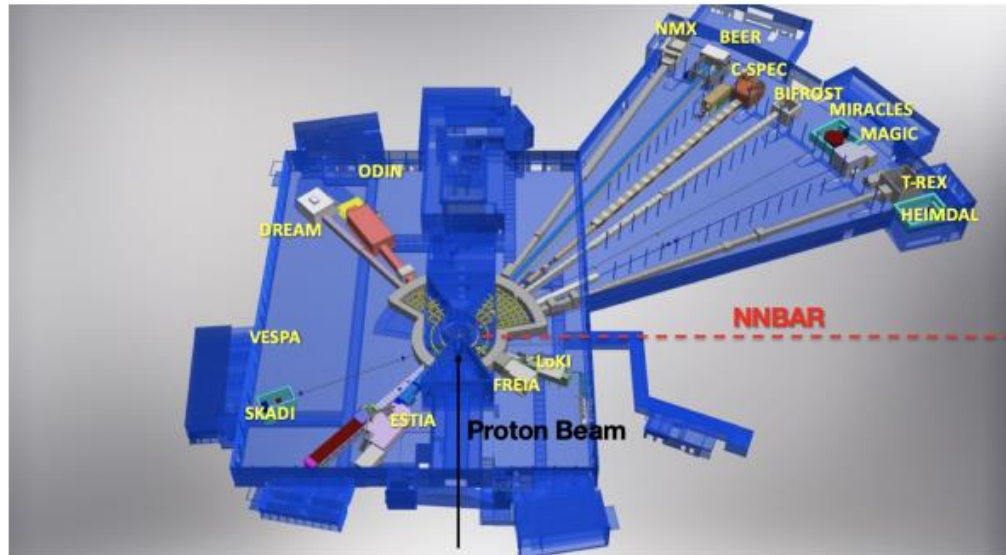


Figure 19: Overview of the ESS instruments and location of the NNBAR experiment.

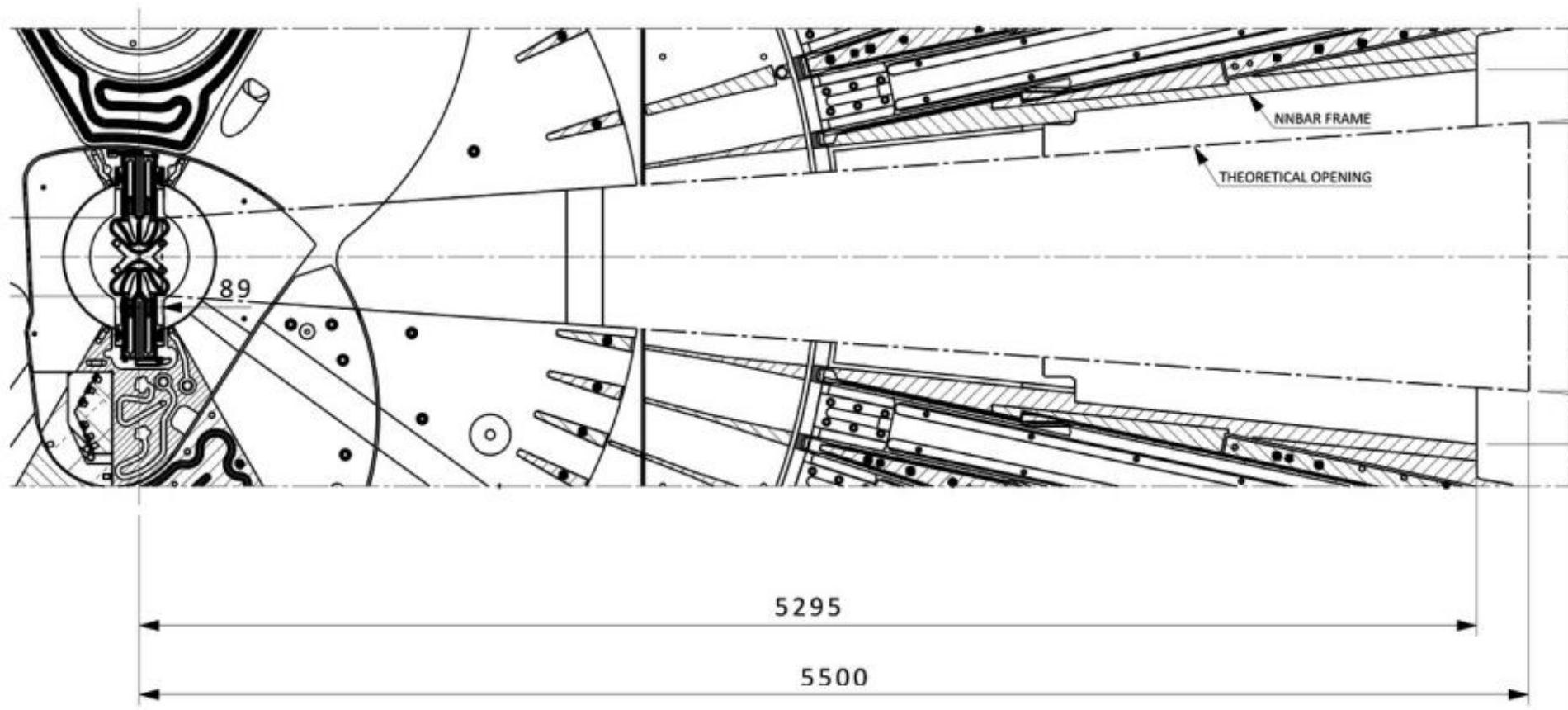


Figure 20: Top view of the NNBAR beamport. Reproduced with permission from Mats Segerup and Rickard Holmberg.



@5.5 m

Figure 21: The ESS Large Beam Port.

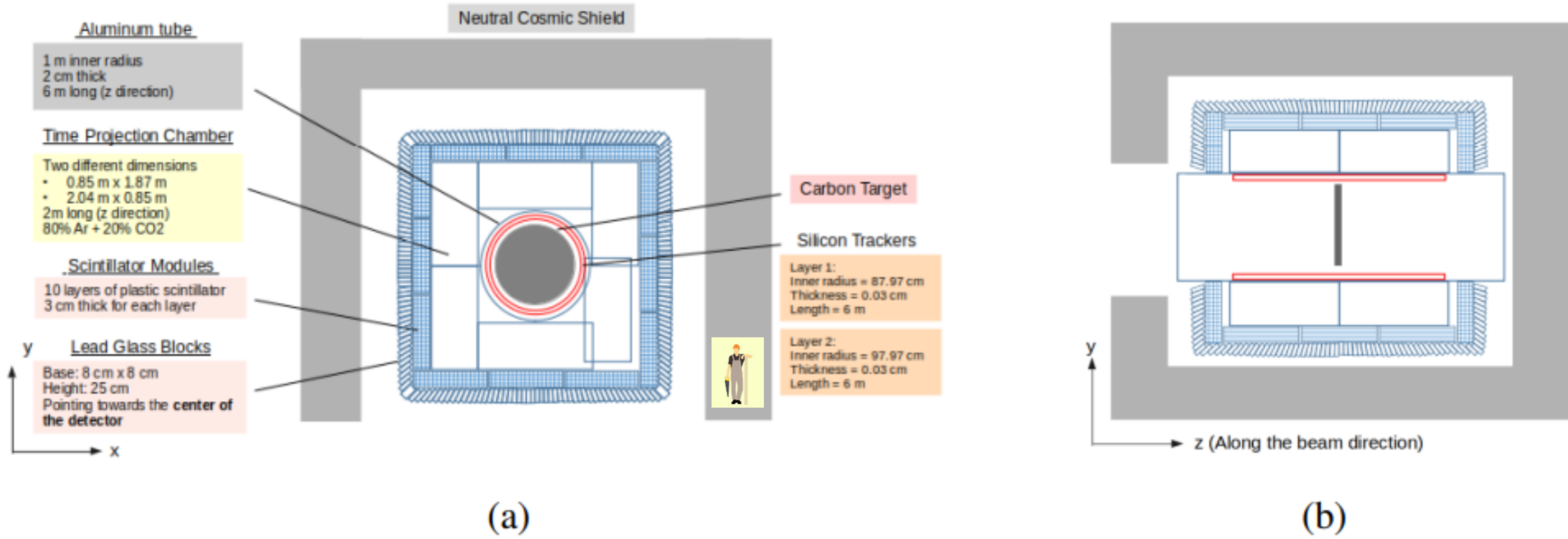


Figure 24: Schematic overview of the NNBAR detector design in the x-y (a) and y-z (b) views.

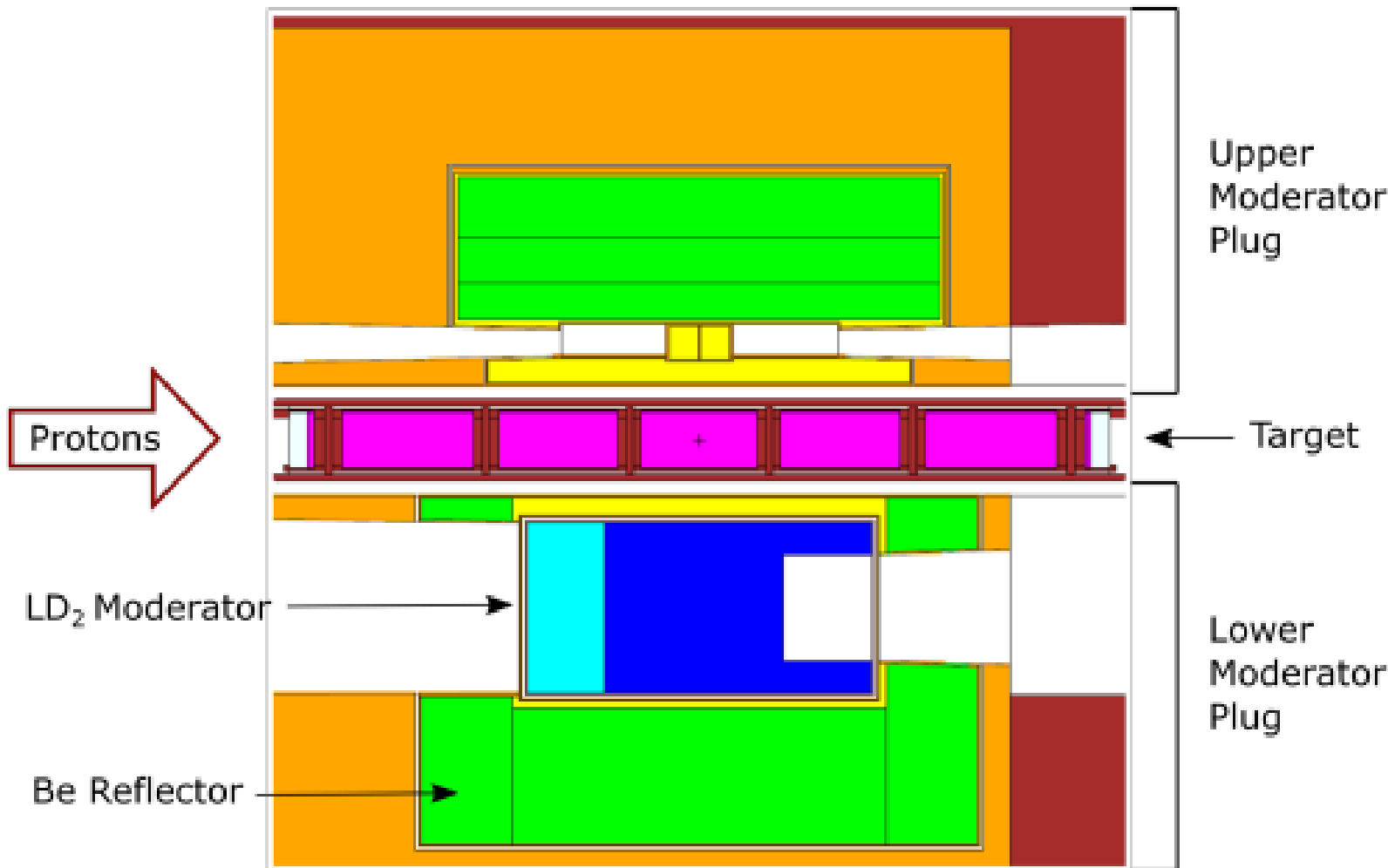


Figure 7: A lower moderator for the ESS.

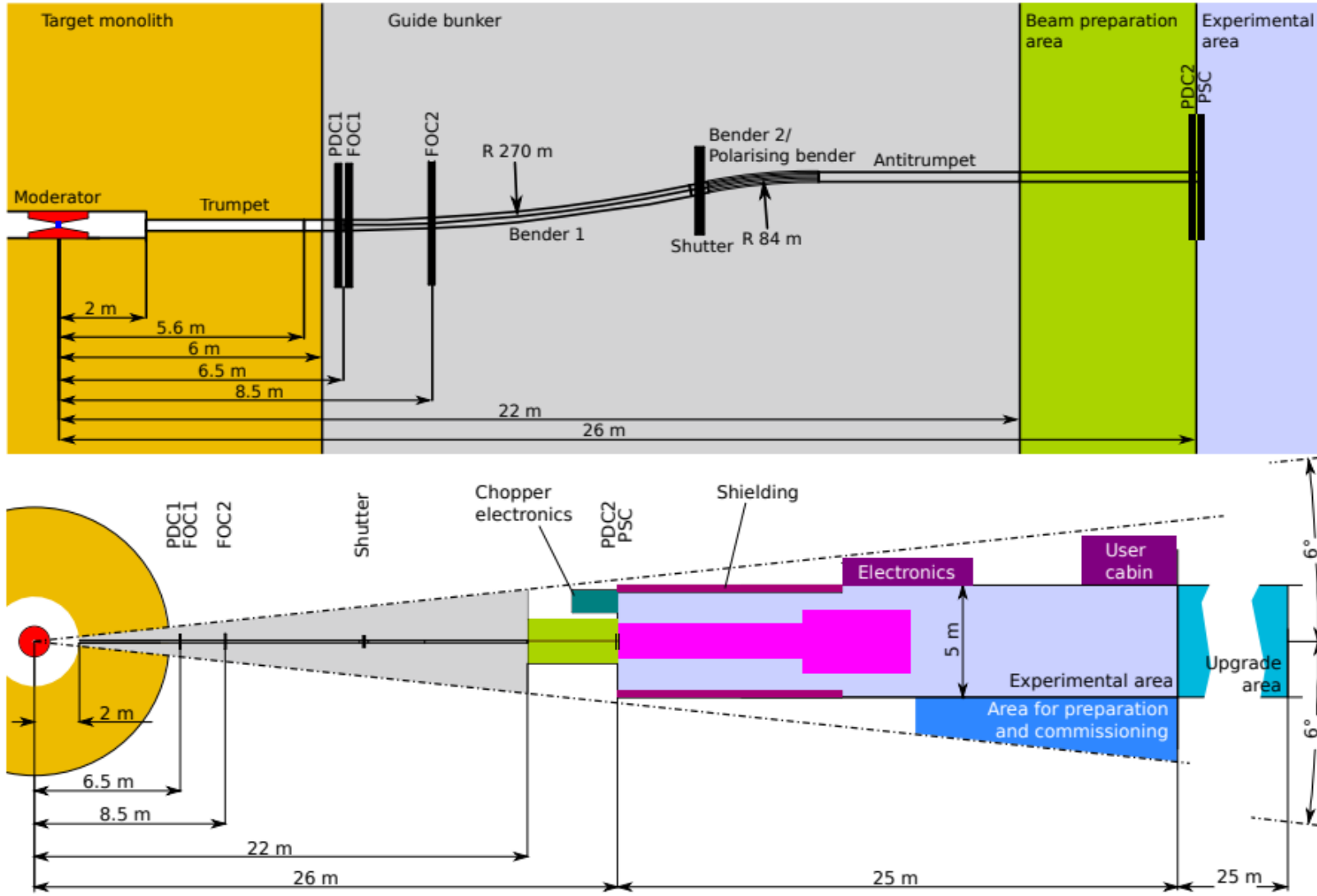


Figure 9: Top: Side view of the proposed ANNI beam line. Trumpet, Bender 1, Bender 2 and Antitrapet assure neutron transport. For experiments with polarised neutrons, Bender 2 is replaced by a polarising bender. PDC1 and PDC2 indicate pulse-defining choppers, FOC1 and FOC2 frame overlap choppers and PSC pulse-suppressing choppers. The vertical scale is stretched by a factor of 4 for better readability. Bottom: Schematic floor plan of the ANNI facility. The magenta area indicates the footprint of PERC with a secondary spectrometer as example for an experiment. The upgrade area is needed for long experiments such as Beam EDM or HIBEAM. Taken from [7].

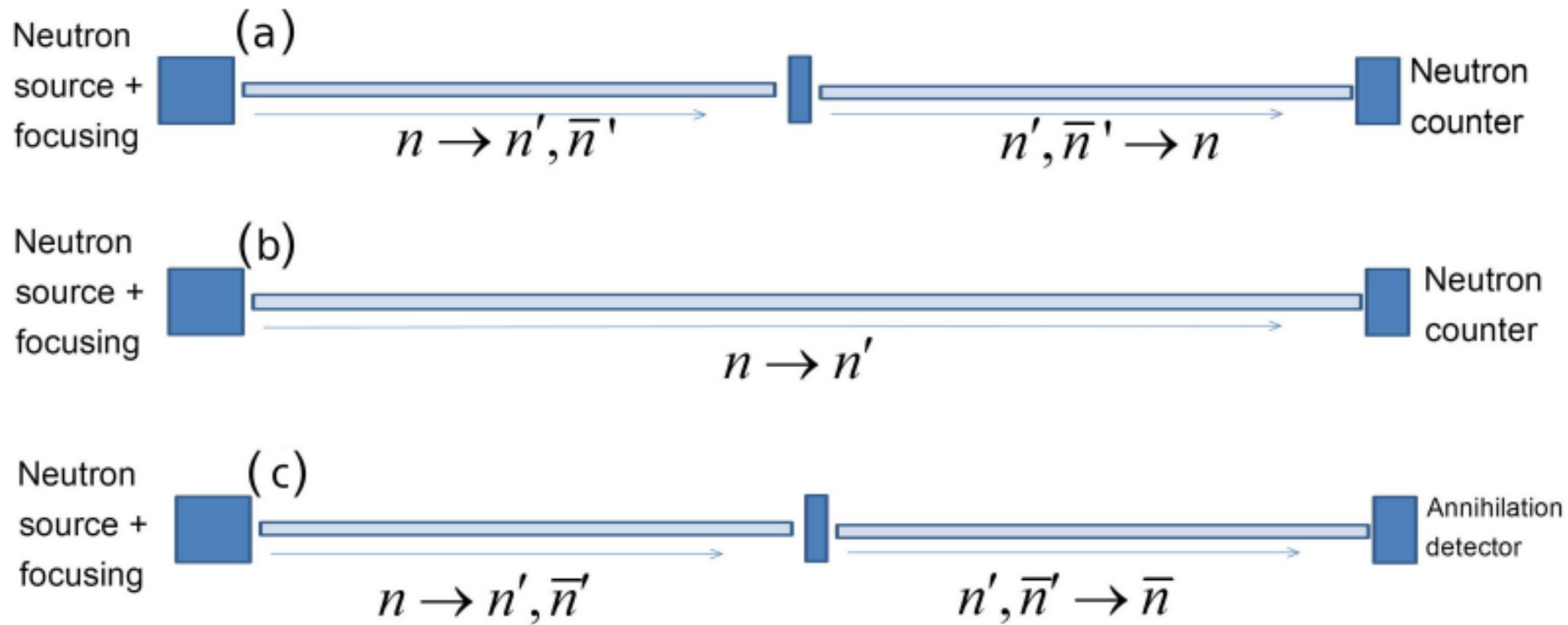


Figure 16: Illustration of the principles of searches for sterile neutron oscillation with neutron beams. Both regeneration (a) ( $n \rightarrow n'$ ) and disappearance (b) ( $n \rightarrow \{\bar{n}, n'\} \rightarrow n$ ) search modes are possible. Another possibility (c) is regenerative in style, though instead leads to further mixing to an antineutron ( $n \rightarrow \{\bar{n}, n'\} \rightarrow \bar{n}$ ), requiring an annihilation detector. Each regeneration mode requires a neutron absorber to be placed at the halfway point of the beamline, preventing all ordinary neutrons from proceeding downbeam while permitting sterile species to pass unencumbered.

2018

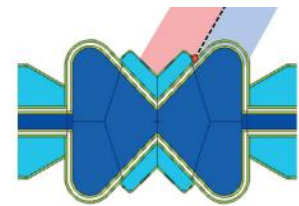
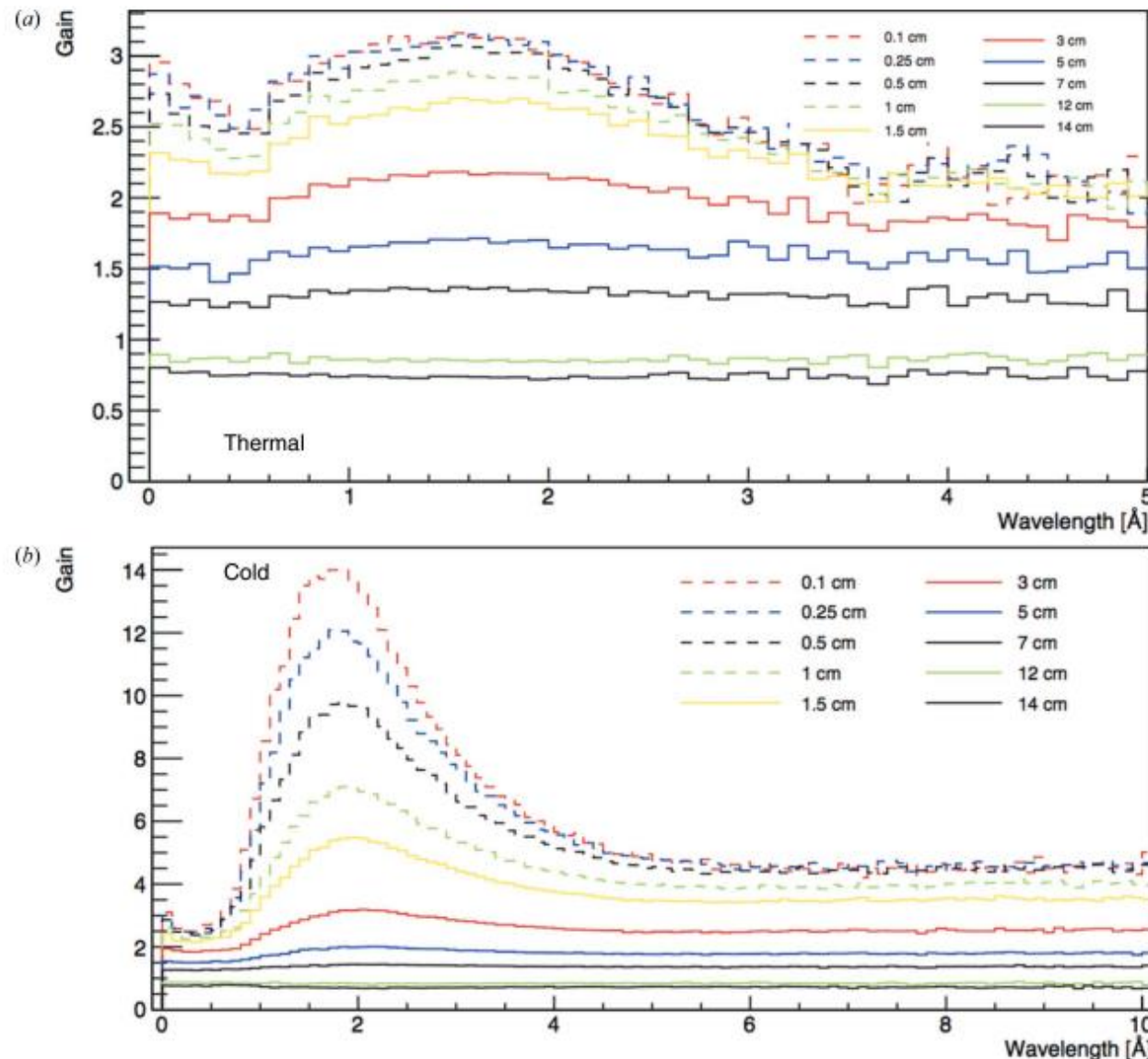


Figure 5

Gain factors for (a) the thermal and (b) the cold moderators (pancake geometry) as a function of wavelength, relative to the 10 cm high pancake moderator, after Zanini *et al.* (2018). As for Fig. 4, the gain factors correspond to a beamport in the centre of the reflector opening and are obtained by averaging over the full moderator height and a width of 6 cm.

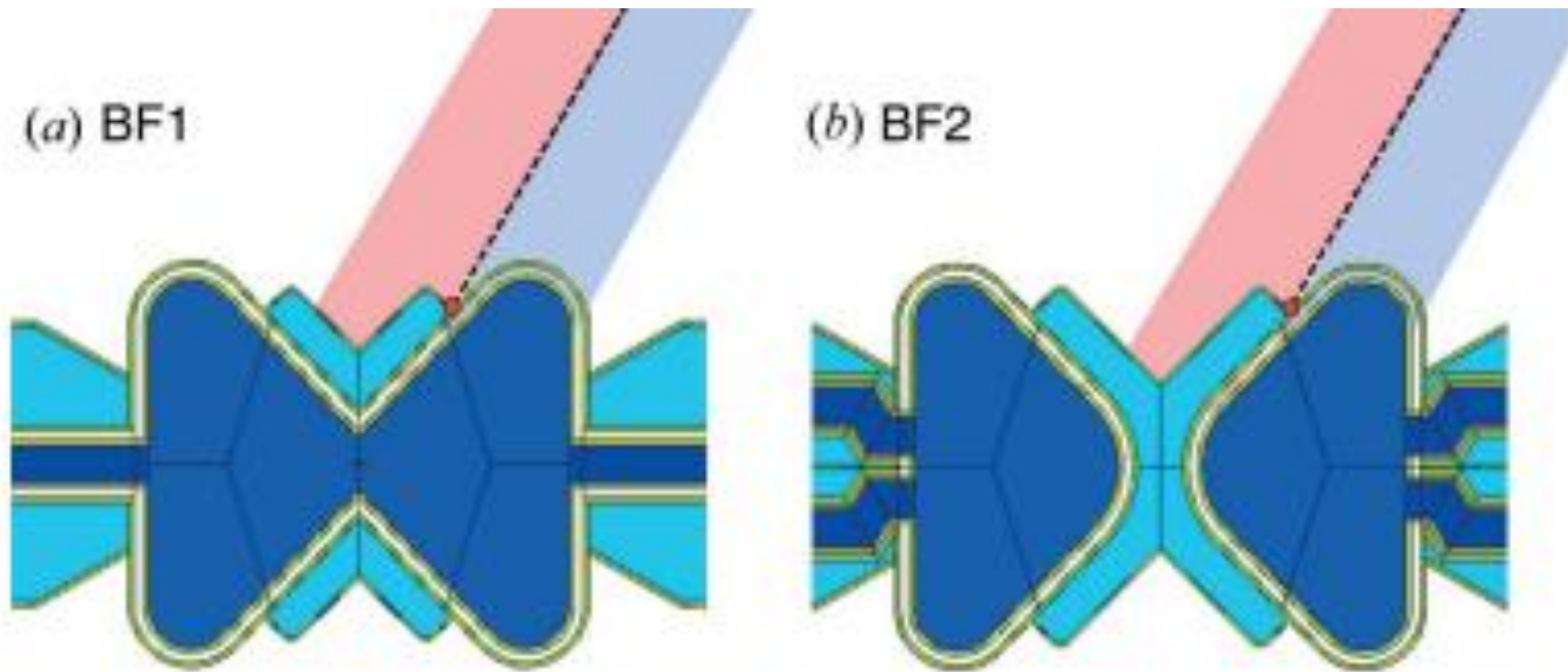


Figure 13

Horizontal slices through the butterfly geometries. (a) BF1 geometry. (b) BF2 geometry. The dark-blue volumes are *para*-hydrogen and the turquoise volumes are water. The proton beam is incident from the right. The focal point for the North sector is indicated with a red spot. The views of the cold and thermal sources are illustrated for the North beamport at  $60^\circ$  with respect to the proton beam, as for Fig. 12.

